Transcript- and annotation-guided genome assembly of the European starling

Katarina C. Stuart[1†], Richard J. Edwards[2†], Yuanyuan Cheng[3], Wesley C. Warren[4], David W. Burt[5], William B. Sherwin[1], Natalie R. Hofmeister[6,7], Scott J. Werner[8], Gregory F. Ball[9], Melissa Bateson[10], Matthew C. Brandley[11], Katherine L. Buchanan[12], Phillip Cassey[13], David F. Clayton[14], Tim De Meyer[15], Simone L. Meddle[16], Lee A. Rollins[1]

[1] Evolution & Ecology Research Centre, School of Biological, Earth and Environmental Sciences, UNSW Sydney, Sydney, New South Wales, Australia

[2] School of Biotechnology and Biomolecular Sciences, UNSW Sydney, Sydney, New South Wales, Australia

[3] School of Life and Environmental Sciences, The University of Sydney, Sydney, New South Wales, Australia

[4] Department of Animal Sciences, Institute for Data Science and Informatics, The University of Missouri, Columbia, Missouri, USA

[5] Office of the Deputy Vice-Chancellor (Research and Innovation), The University of Queensland, Brisbane, Australia

[6] Department of Ecology and Evolutionary Biology, Cornell University, Ithaca, NY 14850

[7] Fuller Evolutionary Biology Program, Cornell Lab of Ornithology, Ithaca, NY 14850

[8] United States Department of Agriculture, Animal and Plant Health Inspection Service, Wildlife Services, National Wildlife Research Center, Fort Collins, Colorado, USA.

[9] Department of Psychology, University of Maryland, College Park, MD 20742 USA

[10] Institute of Neuroscience, Newcastle University, Newcastle upon Tyne, UK

[11] Carnegie Museum of Natural History, Pittsburgh, Pennsylvania, USA

[12] School of Life and Environmental Sciences, Deakin University, Waurn Ponds, VIC, 3228, Australia

[13] Invasion Science & Wildlife Ecology Lab, University of Adelaide, Adelaide SA 5005, Australia

[14] Department of Genetics & Biochemistry, Clemson University, South Carolina 29634

[15] Dept. of Data Analysis & Mathematical Modelling, Faculty of Bioscience Engineering, Ghent University, Ghent, Belgium

[16] The Roslin Institute, The Royal (Dick) School of Veterinary Studies, The University of Edinburgh, Midlothian, EH25 9RG, UK

[†] Joint first authors

Abstract (250 words)

The European starling, *Sturnus vulgaris*, is an ecologically significant, globally invasive avian species that is also suffering from a major decline in its native range. Here, we present the genome assembly and long-read transcriptome of an Australian-sourced European starling (*S. vulgaris* vAU), and a second North American genome (*S. vulgaris* vNA), as complementary reference genomes for population genetic and evolutionary characterisation. *S. vulgaris* vAU combined 10x Genomics linked-reads, low-coverage Nanopore sequencing, and PacBio Iso-Seq full-length transcript scaffolding to generate a 1050 Mb assembly on 1,628 scaffolds (72.5 Mb scaffold N50). Species-specific transcript mapping and gene annotation revealed high structural and functional completeness (94.6% BUSCO completeness). Further scaffolding against the high-quality zebra finch (*Taeniopygia guttata*) genome assigned 98.6% of the assembly to 32 putative nuclear chromosome scaffolds. Rapid, recent advances in sequencing technologies and bioinformatics software have highlighted the need for evidence-based assessment of assembly decisions on a case-by-case basis. Using *S. vulgaris* vAU, we demonstrate how the multifunctional use of PacBio Iso-Seq transcript data and complementary homology-based annotation of sequential assembly steps (assessed using a new tool, SAAGA) can be used to assess, inform, and validate assembly workflow decisions. We also highlight some counter-intuitive behaviour in traditional BUSCO metrics, and present BUSCOMP, a complementary tool for assembly comparison designed to be robust to differences in assembly size and base-calling quality. Finally, we present a second starling assembly, *S. vulgaris* vNA, to facilitate comparative analysis and global genomic research on this ecologically important species.

Keywords: *Sturnus vulgaris*, genome assembly, genome assessment, genome annotation, full-length transcripts

1. Introduction

The European starling (*Sturnus vulgaris*) is a globally invasive passerine that was deliberately introduced during early European acclimatisation efforts into North America, Australia, New Zealand, and South Africa during the mid-late 19th century (Feare 1985). More recently, the species was accidentally introduced into South America (Palacio et al. 2016). Since these introductions the invasive ranges of the starling have been expanding, with the species now occupying a range in excess of 38,400,000 km^2 globally (BirdLife International 2020), posing threats to the economics and health of the agriculture industry, as well as local biodiversity (Bomford & Sinclair 2002; Koch et al., 2009; Palacio et al., 2016; Linz et al., 2017). Recent molecular ecology studies of individuals from the invasive ranges of North America, Australia, and South Africa report that these populations are undergoing rapid and independent evolution in response to novel local selection pressures (Phair et al., 2018; Hofmeister et al., 2019; Bodt et al., 2020; Stuart et al., 2020), a common phenomenon in many invasive populations (Prentis et al., 2008). This suggests the starling has a flexible invasion strategy, potentially enabling colonisation of ecosystems vastly different from those in their native range.

Despite their invasive range success, European starlings are increasingly of ecological concern within their native range (Rintala et al., 2003; Robinson et al., 2005). High densities of native range starlings have traditionally been supported by cattle farming across Europe, because starlings preferentially feed in open grasslands, and benefit from invertebrates in overturned soil produced by livestock grazing (Coleman 1977). A shift towards modern indoor cattle rearing processes across Europe may contribute to the decline in starling numbers, which has been a concern since the 1980s (Wretenberg et al., 2006). This decline is reflected globally, with starling and other avifauna numbers decreasing sharply over the last few decades (Spooner et al., 2018; Rosenberg et al., 2019), though this may be further

amplified for starling populations subjected to control strategies to reduce their economic impact (Linz et al., 2007). The biological and ecological importance of this species is evident from its prolific use in research, as it is the most studied non-domesticated passerine (Bateson & Feenders 2010). It is evident that future research on the European starling will focus on identifying patterns of evolutionary diversification, as well as investigating genes associated with invasion success. Such research provides important information for the improvement of control measures and may also provide insight into recovery and dispersive potential in other species that would benefit global conservation efforts. For this, a high-quality, annotated reference genome is essential.

Once reliant on large consortia, assembling high-quality reference genomes for genetic analyses is now commonplace. Nevertheless, *de novo* assembly of non-model organism genomes still poses many challenges. Best practices may have not been established for the study species/data, and basic information such as genome size, repeat landscape, and ploidy may be unknown. Furthermore, high-quality references can be generated in multiple ways, which can serve varied research purposes. Rapid developments in both sequencing technology and bioinformatics methods can quickly outdate benchmarking attempts. Whilst not always documented in final publications, the standard practice for non-model species genomes is to select from multiple assemblies generated using different assembly methods, none of which is universally best (Rhie et al., 2020; Whibley et al., 2020). This complexity can be magnified further when sequencing occurs across multiple technology platforms that may be combined and utilised in different ways (Jayakumar & Sakakibara 2019; Kono & Arakawa 2019). The challenge is then to select the best combination of tools and assembly decisions, based on the quality of the genome assemblies produced.

A multitude of tools and approaches are available for genome assembly assessment, though some may not be applicable or feasibly implemented for a particular

111 species/assembly and/or the data available (e.g. Bradnam et al., 2013; Hunt et al., 2013; Yuan
112 et al., 2017). Common approaches employed to guide genome assembly decisions focus on
113 contiguity (how continuous the assembled sequences are) and completeness (whether the
114 assembly contains all the genetic information for that species). Two such approaches are
115 assembly statistics (e.g., contig/scaffold counts, and L50/N50 statistics of the number and
116 shortest length of sequences needed to cover 50% of the assembly) and "Benchmarking
117 Universal Single Copy Orthologs" (BUSCO) estimates of genome completeness (Simão et
118 al., 2015). Assembly statistics are very quick to generate and easy to understand, but
119 interpretation can be challenging due to hidden assembly errors and artefacts, which can
120 create false signals. BUSCO assesses the presence or absence of highly conserved lineage-
121 specific genes but is limited to a set of common single-copy genes that may represent easier
122 regions of the genome to sequence and assemble based on current bioinformatics
123 technologies. Furthermore, BUSCO analysis is vulnerable to unpredictable misreporting of
124 presence/completeness for specific genes as a consequence of assembly differences elsewhere
125 in the genome (Edwards et al., 2018; Edwards 2019; Field et al., 2020; Edwards et al., 2021).
126 In addition to the above drawbacks, these methods do not explicitly test the genome
127 assembly's ability to perform the role for which it was intended (e.g., to serve as a reference
128 genome for specific genomic analysis).

129 Here, we present the first official release of the European starling draft genome, *S.*
130 *vulgaris* vAU. This assembly represents the first synthesis of species-specific full-length
131 transcripts, together with genomic data for this species. In this paper, we complement genome
132 statistics and BUSCO completeness with transcriptome- and annotation-based assessments
133 that help determine genome assembly quality and completeness in the absence of a reference
134 genome to benchmark against. We demonstrate how full-length transcripts can be utilised in
135 genome assembly scaffolding and assessment, in addition to transcriptome construction and

136 annotation. We show how BUSCOMP (https://github.com/slimsuite/buscomp) can help avoid
137 over-interpretation or misinterpretation of small differences in BUSCO completeness. We
138 also explore how lightweight homology-based annotation by GeMoMa (Keilwagen et al.,
139 2018), can be used as an assembly assessment using a new tool, SAAGA
140 (https://github.com/slimsuite/saaga). Finally, we compare the Australian *S. vulgaris* vAU
141 assembly (GCF_ JAGFZL000000000) with an additional (short read) assembly of a North
142 American bird, *S. vulgaris* vNA (GCF_001447265.1), enabling reference-specific biases to
143 be identified in future starling genomics studies.
144
145 **2. Material and Methods**
146 **2.1 Genome assembly and scaffolding**
147 The *S. vulgaris* vAU genome assembly used 10x Chromium linked reads and low coverage
148 ONT long reads (Appendix 1: Genomic DNA sample collection, gDNA extraction, and
149 sequencing), and was produced via eight assembly steps (Fig. 1). The 10x reads were
150 assembled into an initial diploid assembly using SUPERNOVA (v2.1.1) (Weisenfeld et al.,
151 2017) with barcode fraction and reads subsample calculated following SUPERNOVA best
152 practices for a genome size based on k-mer counts calculation by JELLYFISH v2.2.10 (Marçais
153 & Kingsford 2011) (parameters: bcfrac = 0.8, maxreads = 550 million, Supplementary
154 Materials: Appendix 2, Validation of SUPERNOVA genome size prediction using JELLYFISH,
155 Supplementary Materials: Fig. S1). This assembly was then split into non-redundant primary
156 and alternative haploid assemblies using DIPLOIDOCUS (parameters: runmode= diphapnr)
157 (v0.9.5) (https://github.com/slimsuite/diploidocus). First, both SUPERNOVA pseudohap2
158 assemblies were combined and any sequences lacking definitive base calls (100% Ns) were
159 removed. Remaining scaffolds were size-sorted and gaps reduced in size to a maximum of 10
160 Ns then subject to an all-by-all search with MINIMAP2 (v2.17) (Li 2018) (--cs -p 0.0001 -x

asm20 -N 250). (Note that gap size reduction is used for MINIMAP2 searching only, and the non-redundant pseudodiploid assembly produced has the same gap sizes as generated by SUPERNOVA.). Any sequences that were 100% contained within another sequence were removed. Where two or more scaffolds had an 100% identical sequence, only one was kept. Scaffolds are then matched into haplotig pairs based on their SUPERNOVA names. Where a single haplotig is found, it is assigned as diploid, under the assumption that the two original haplotigs were identical with one removed, and added to the primary assembly. (Note: it is possible that only one parent had this scaffold, e.g., a sex chromosome scaffold or structural variant.). If two haplotigs are identified, the longest is assigned to the primary assembly and the shorter to the alternative assembly. The primary assembly should therefore contain an entire haploid copy of the genome, whilst the alternative assembly contains the subset of scaffolds with heterozygous haplotigs.

The primary haploid assembly produced by DIPLOIDOCUS was scaffolded using the filtered ONT reads using the program SSPACE-LONGREAD (v1-1) (Boetzer & Pirovano 2014). The filtered ONT reads were then used to gap-fill the assembly using GAPFINISHER (v1.0) (Kammonen et al., 2019). Clustered high quality Iso-Seq reads (see section 2.2 cDNA analysis) were then used for a secondary round of scaffolding using L_RNA_SCAFFOLDER (Xue et al., 2013). Paired-end 10x linked reads were processed with 10X Genomics LONG RANGER (v2.2) and mapped onto this scaffolded assembly using BWA *mem* before error correction of SNPs and indels using PILON (v1.23) (Walker et al., 2014) (parameters: --diploid –fix all settings). To validate the scaffolds, the assembly was analysed using the BREAK10X toolkit in SCAFF10X (v3.1) (https://github.com/wtsi-hpag/Scaff10X). The assembly was further checked for assembly artefacts and contamination using DIPLOIDOCUS (parameters: runmode=purgehaplotig & runmode=vecscreen (ref); runmode=DipCycle was tested yet discarded due to over-pruning, see Supplementary Materials: Fig. S2) (v0.9.5).

Avian species are characterised by distinctive and constrained karyotypes, generally comprised of approximately 10 macrochromosomes and approximately 30 indistinguishable microchromosomes (Griffin et al., 2007; O'Connor et al., 2019), a pattern to which the *S. vulgaris* genome conforms (Calafati & Capanna 1981). Therefore, we aligned our assembly to the chromosome scale assembly of zebra finch (Taeniopygia guttata) (NCBI= GCF_008822105.2) (Balakrishnan et al., 2010) using SATSUMA2 (https://github.com/bioinfologics/satsuma2) to create putative chromosomes assuming orthology. This assembly formed the final updated draft genome we present for the species: *Sturnus vulgaris* vAU.

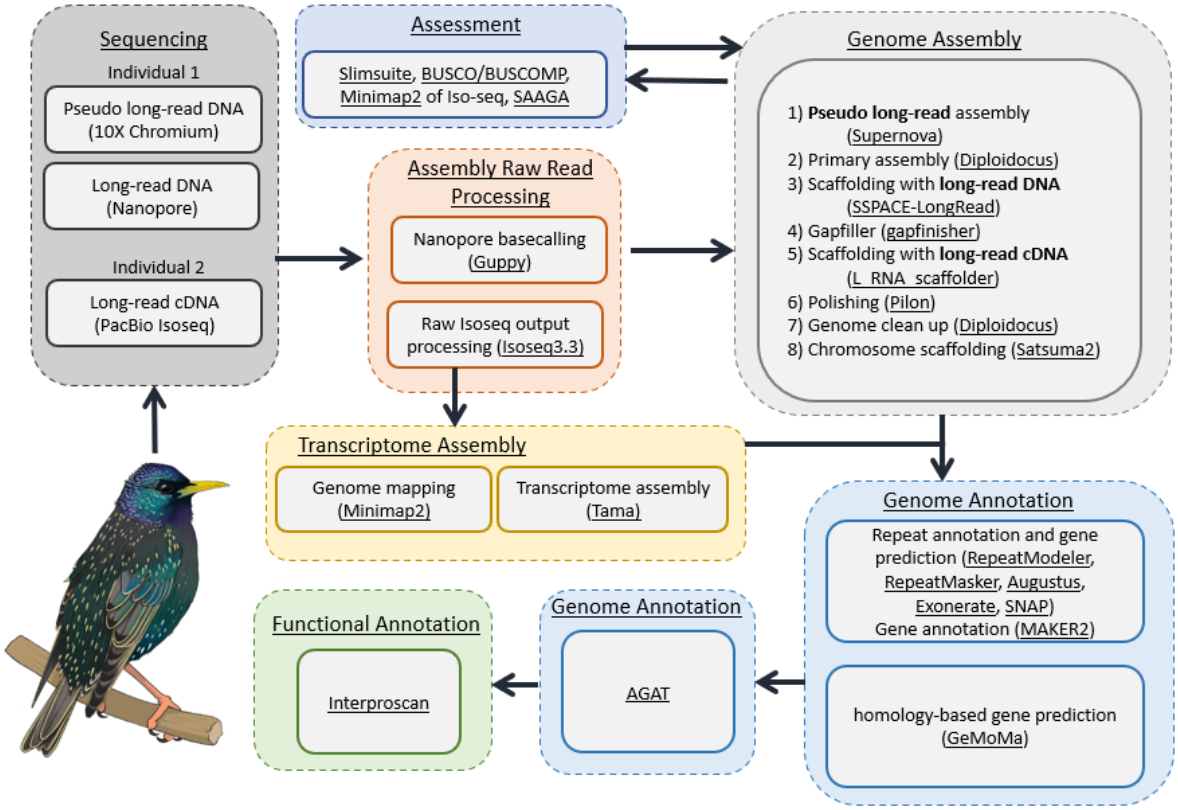

Figure 1: Workflow for genome assembly and annotation. A summary of all the experimental methods used for sequencing, genome assembly, transcriptome assembly, genome annotation, and functional annotation, with programs used underlined.

2.2 Transcriptome assembly and analysis

Raw PacBio Iso-Seq whole transcript reads (Appendix 3: Transcriptome sample collection, RNA extraction, and sequencing) were processed using the protocol outlined in SMRT LINK (v9.0) (PacBio, California, United States). Briefly, this involved generating Circular Consensus Sequences (CCS) using CCS (v4.2.0), which were then processed using Lima (v1.11.0) for primer removal and demultiplexing. The reads were further processed (PolyA tail minimum length = 8) and clustered using ISO-SEQ (v3.3). The high quality clustered Iso-Seq reads were then aligned to the reference genome (see section 2.1 Genome assembly and scaffolding) using minimap2 (v2.17) (Li 2018), before further processing using TAMA collapse (Kuo et al., 2020) (settings -a 100 -z 30 -sj sj_priority -lde 5). Both these steps were assessed using BUSCO (v3.0.2b) (Simão et al., 2015) (parameters: aves lineage, transcriptome mode), alongside a short read transcriptome produced from *S. vulgaris* liver RNA (Richardson et al., 2017), as well as other available avian Iso-seq transcriptomes (Workman et al., 2018; Yin et al., 2019).

2.3 Genome annotation and functional annotation

Each stage of genome assembly was annotated using GEMOMA v1.7.1 (Keilwagen et al., 2018) using the 26 avian genome annotations available on Ensembl at the time this analysis was conducted (Supplementary Materials, Table S1) and with the high quality clustered Iso-seq, as RNA evidence. The GEMOMA *GeMoMaPipeline* function was run to complete the full pipeline with a maximum intron size of 200 kb (parameters: tblastn=false GeMoMa.m=200000 GeMoMa.Score=ReAlign AnnotationFinalizer.r=SIMPLE pc=true o=true).

The final *S. vulgaris* vAU genome assembly was also annotated with MAKER2 (Holt & Yandell 2011) (BLAST+ v2.9 (Camacho et al., 2009), AUGUSTUS v3.3.2 (Stanke & Morgenstern 2005), EXONERATE v2.2.0 (Gs & E 2005), REPEATMASKER v4.0.7 (Smit et al.,

2013), REPEATMODELER v1.0.11 (Flynn et al., 2020), and SNAP v0.15.4 (Korf 2004) using repeat-filtered Swiss-Prot protein sequences (downloaded Aug 2018) (UniProt Consortium 2019). A custom AUGUSTUS species database was created by running BUSCO using the Optimization mode Augustus self-training mode (--long), using the aves database for lineage. MAKER2 was run using the recommended protocol, including generation of a repeat library, and with the TAMA-processed Iso-Seq data included as primary species transcript evidence, and the pre-existing short read liver transcript data (Richardson et al., 2017) provided as alternate transcript evidence in the first iteration of the MAKER2 annotation process. We ran MAKER2 for a total of three training runs, using the hidden Markov models (HMMs) produced from SNAP training in each subsequent run. *Ab initio* genes were not retained in the final annotation model to produce high quality and conservative gene predictions. GEMOMA and MAKER2 annotations for the final *S. vulgaris* vAU assembly were combined using the AGAT *agat_sp_merge_annotations* function to produce the final annotation. Functional annotation of protein-coding genes were generated using INTERPROSCAN 5.25–64.0 (parameters: -dp -goterms -iprlookup -appl TIGRFAM, SFLD, Phobius, SUPERFAMILY, PANTHER, Gene3D, Hamap, ProSiteProfiles, Coils, SMART, CDD, PRINTS, Pro SitePatterns, SignalP_EUK, Pfam, ProDom, MobiDBLite, PIRSF, TMHMM). BLAST was used to annotate predicted genes using all Swiss-Prot proteins (parameters: -evalue 0.000001 -seg yes -soft_masking true -lcase_masking -max_hsps). Annotation summaries were generated using the AGAT *agat_sp_functional_statistics.pl* script, BEDTOOLS was used to calculate gene coverage statistics. Gene ontology terms were assigned using WEGO v2.0 (Ye et al., 2018).

2.4 Annotation assessment using SAAGA: Summarise, Annotate & Assess Genome Annotations

SAAGA (Summarise, Annotate & Assess Genome Annotations) (v0.5.3) (https://github.com/slimsuite/saaga) was used to assess annotation quality and compare predicted proteins to the repeat- and transposase-filter Swiss-Prot protein sequences used for MAKER2 annotation (above). SAAGA performs a reciprocal MMseqs2 (Steinegger & Söding 2017) search of annotated proteins against a (high-quality) reference proteome, identifying best hits for protein identification and employing coverage ratios between query and hit proteins as a means of annotation assessment to generate summary statistics, including:

- **Protein length ratio.** The length ratio of the annotated proteins versus its top reference hit
- **F1 score.** An annotation consistency metric calculated using the formula:

$$(2 \times \text{PROTCOV} \times \text{REFCOV}) / (\text{PROTCOV} + \text{REFCOV})$$

  where PROTCOV is the proportion of the annotated protein covered by its best reference protein hit, and REFCOV is the proportion of the best reference protein hit covered by the annotated protein.
- **Completeness.** The summed percentage coverage of reference proteome.
- **Purity.** The summed percentage reference coverage of the annotated proteome.
- **Homology.** The percentage of annotated genes with any hit in reference.
- **Orthology.** The percentage of annotated genes with reciprocal best hits in reference.
- **Duplicity.** The mean number of annotated genes sharing the same best reference hit.
- **Compression.** The number of unique annotated genes that were the top hit for reference proteins, divided by the total number of reference proteins with a hit.
- **Multiplicity.** The ratio of total number of annotated genes to reference proteins.

For protein length ratio and F1 score, values close to 1 means that the query protein closely matches the length of the hit protein, indicating high fidelity of the gene prediction model and underlying assembly. The remaining metrics will be closer to 1 (or 100%) for complete

278 annotations and assemblies without duplications, akin to BUSCO scores. Although the
279 maximum achievable value for these metrics will generally be unknown, comparative values
280 can be used to assess improvement in assembly and/or annotation.

281 SAAGA scores may be used to compare alternate annotations of the same assembly,
282 or to compare alternative assemblies in conjunction with consistent annotation. Low genome
283 contiguity, misassembles, or frameshifting indels will affect the quality of predicted genes,
284 with poorer assemblies reporting more fragmented or truncated genes. This approach has
285 been facilitated by the rapid homology-based gene prediction program GeMoMa, which uses
286 reference genome annotation to predict protein-coding genes in the target genome. The
287 program can be run from one line of code and may be parallelised to run much faster than
288 other annotation software (e.g., Maker2). The ease of this annotation tool opens the way for
289 conducting annotations for the purpose of assessment on sequential or even competing
290 genome annotation steps. Assessing the quality of protein-coding region predictions will help
291 ensure the final genome assembly can produce a high-quality annotation. Here, we used the
292 repeat-filtered Swiss-Prot database used in annotation, and the *Gallus gallus* reference
293 proteome (UP000000539_9031), to assess predicted protein quality and annotated proteome
294 completeness.

295 **2.5 Genome assembly completeness assessment**

296 Assembly contiguity and completeness was assessed for sequential genome assembly steps of
297 the *S. vulgaris* vAU assembly and compared to existing passerine chromosome level
298 assemblies available on NCBI, including the *S. vulgaris* vNA assembly (Assembly accession
299 GCF_001447265.1, Supplementary Material: Appendix 4, Assembly and annotation of the *S.*
300 *vulgaris* vNA genome version).

301 **2.5.1 BUSCO and BUSCOMP assembly completeness assessment**

Genome completeness was estimated using BUSCO (v3.0.2b, genome mode, aves lineage). BUSCO resulted were collated across all assemblies using BUSCOMP v0.10.1 (https://github.com/slimsuite/buscomp). BUSCOMP collated BUSCO outputs across all genome assembly stages and compiled a maximal non-redundant set of 4727 complete BUSCOs found at single copy in at least one assembly. Compiled BUSCO predicted gene sequences were mapped onto each assembly to be rated with MINIMAP2 V2.17 (Li 2018) and re-scored in terms of completeness, thereby providing a robust and consistent means of assessing comparable completeness across assemblies of the same genome.

2.5.2 PacBio Iso-Seq completeness assessment

The PacBio Iso-Seq reads were mapped on to genome assemblies using MINIMAP2 (parameters: -ax splice -uf --secondary=no --splice-flank=no -C5 -O6,24 -B4) (Li 2018) and the number of Iso-Seq transcripts mapping on to each assembly, and their corresponding mapping quality, was calculated.

2.5.3 KAT k-mer completeness assessment

The final genome assembly completeness was assessed by examining the read k-mer frequency distribution with different assembly copy numbers based on the 10x Chromium linked reads using K-MER ANALYSIS TOOLKIT (KAT) v2.4.2 (Mapleson et al., 2017) (30 bp trimmed for R1 reads, and 16 bp trimmed for R2 reads).

2.6 Additional genome statistics

The Iso-Seq and final annotation transcript density, final annotation gene density, global SNP variant density (based on a whole genome data set of 24 individuals from United Kingdom, North America, and Australia, N=8 (Hofmeister et al., 2020), and GC-content were calculated in sliding windows of width 1 Mb using BEDTOOLS V 2.27.1 (Quinlan & Hall 2010), and plotted across the largest 32 scaffolds in our final genome assembly (representing

more than 98% of the total assembly captured on putative chromosomes orthologous to other avian chromosomes) using CIRCLIZE (v 0.4.9) (Gu et al., 2014).

2.7 Genome assembly correction

NCBI VecScreen flagged possible bacterial and adapter contamination in the final *S. vulgaris vAU* assembly, which was missed by earlier contamination screening steps. An updated version of DIPLOIDOCUS (runmode vecscreen) was run to mask shorter adapter sequences and flag additional organism contaminates (screenmode=purge vecmask=27). Four related bacterial strains (Delftia acidovorans SPH-1, Acidovorax sp. JS42, Alicycliphilus denitrificans K601, Paraburkholderia xenovorans LB400) were identified, and so GABLAM v2.30.5 (Davey et al., 2006) was used to search these four genomes against the final assembly, and purge small contigs (<5,000 bp) that contained sequence matches (285 short contigs excluded). For larger scaffolds that contained possible embedded contaminated sequences, the high quality ONT reads were mapped using Minimap2 over the regions. For those contaminated sites that had Nanopore reads spanning the contaminated region, the sequences were masked, and for those lacking nanopore support, the scaffold was split and/or trimmed to remove the contaminating sequence (seq 4 trimmed, seq 12 and 31 split into chromosome and unplaced scaffold). Finally, gaps of unknown size were standardised to 100 bp, and mitochondrial genome insertions into the nuclear genome were assessed using NUMTfinder (https://github.com/slimsuite/numtfinder) (Edwards et al., 2021) (none located). This paper primarily analyses S. vulgaris vAU1.0 (which we refer to has *S. vulgaris* vAU), while the final NCBI release (accession = JAGFZL000000000) is explicitly referred to as *S. vulgaris* vAU1.1 when relevant.

2.8 BUSCO versus BUSCOMP performance benchmarking

BUSCO-containing scaffolds from the DIPLOIDOCUS primary haploid SUPERNOVA assembly of *Sturnus vulgaris* vAU were extracted into a reduced genome ‘pribusco’ assembly for

additional BUSCO and BUSCOMP benchmarking (Supplementary Materials: Fig. S3). BUSCO v3.0.2b (Simão et al., 2015) (HMMER v3.2.1 (Wheeler & Eddy 2013), AUGUSTUS v3.3.2 (Stanke & Morgenstern 2005), BLAST+ v2.2.31 blast(Camacho et al., 2009), EMBOSS v6.6.0 (Rice et al., 2000)) was run in genome mode with the aves_odb9 dataset (n=4915) on: the non-redundant pseudodiploid ('dipnr'), primary ('pri') and alternative ('alt') assemblies; BUSCO-containing scaffolds from the primary assembly ('pribusco'); a reverse-complemented copy ('revcomp'), combined with 'pribusco' to make a 100% duplicate assembly ('duplicate'); a direct copy ('copy') combined with 'duplicate' to make a triplicated assembly ('triplicate'); three randomly shuffled versions of 'pribusco' ('shuffle1', 'shuffle2', 'shuffle3'), added in combination to `pribusco` to generate datasets of increasing assembly size without increasing duplication levels ('2n', '3n' and '4n'); ten straight repeats of the `pribusco` run (`rep0` to `rep9`). All BUSCO results were processed with BUSCOMP v0.11.0 (MINIMAP2 v2.17). In addition to the full BUSCOMP analysis of all runs, the following subsets were grouped for analysis (Supplementary File 1, BUSCO v3 BUSCOMP output):

- Pseudodip: 'dipnr', 'pri' and 'alt'. (Haploid versus diploid assemblies.)
- Core: 'dipnr', 'pri', 'alt', 'pribusco' and 'revcomp'. (Assembly filtering and manipulation.)
- Duplication: 'copy', 'duplicate', 'triplicate'. (Duplicating scaffolds.)
- Size: 'shuffle1', 'shuffle2', 'shuffle3', '2n', '3n', '4n'. (Increasing assembly size without duplication.)
- Replicates: 'rep0' to 'rep9'.

The same analysis was repeated with BUSCO v5.0.0 (Simão et al., 2015) (SEPP v4.3.10 (Mirarab et al., 2012), BLAST v2.11.0 (Camacho et al., 2009), HMMer v3.3 (Wheeler & Eddy 2013), AUGUSTUS v3.3.2 (Stanke & Morgenstern 2005), PRODIGAL v2.6.3 (Hyatt et

al., 2010), METAEUK v20200908 (Levy Karin et al., 2020)) and the aves_odb10 dataset (n=8338).

3. Results

3.1 *Sturnus vulgaris* vAU genome assembly

Genome assembly of *Sturnus vulgaris* vAU combined three different sequencing technologies for *de novo* genome assembly (10x Genomics linked reads, ONT long reads, and PacBio Iso-Seq full length transcripts) (Table 1), before a predicted reference-based scaffolding to the chromosome level using the high-quality reference assembly of *T. guttata* (NCBI REF: GCF_008822105.2). Approximately 109 Gb (97x coverage) of 10x linked read data (subsampled during assembly to 56x based on the estimated genome size of 1.119 Gb, barcode subsampling of 80%) were assembled with SUPERNOVA (v2.1.1) (Weisenfeld et al., 2017) (step 1) and converted to a primary haploid assembly (step2). We generated approximately 8 Gb of raw genomic reads using an ONT minion, which were reduced to 5 Gb after stringent filtering (Table 1). These data were used to scaffold the genome (step 3) and gap-fill (step 4), reducing the total number of scaffolds from 18,439 to 7,856, increasing the scaffold N50 from 1.76 Mb to 7.12 Mb, and decreasing the scaffold L50 from 146 to 39 (Supplementary Materials: Fig. S4). These measures were further improved after Iso-Seq scaffolding (step 5) (7,776 scaffolds, N50 7.12 Mb, and L50 38), followed by Pilon polishing using 10x linked reads (step 6). Finally, following haplotig removal (step 7), chromosomal alignment against the *T. guttata* reference genome (step 8) reduced the final number of scaffolds to 1,628 (N50 72.5 Mb, and L50 5) (Supplementary Materials: Fig. S4), with 98.6% of the assembly assigned to 32 putative nuclear chromosome scaffolds. While no whole mitochondrial genome insertions were found, 27 smaller mitochondrial pseudogenes (NUMTs) were located in *S. vulgaris* vAU1.1, with scaffold 31 (corresponding to the Z chromosome) containing the highest amount (Table S2).

Table 1: Summary of sequencing data for *Sturnus vulgaris* vAU genome assembly and annotation

Genetic Data	Platform	Library	Library length/Mean Insert Size (kb)	Mean raw Read Length (bp)	Number of Reads	Number of bases (Gb)
gDNA	Hiseq X Ten	Paired-end 10x Chromium	51.7kb	150	361,950,449	108.58
gDNA	ONT MinION	Ligation	47kb	6,417	1,225,865	7.865
cDNA	PacBio	Iso-Seq	Full transcripts (brain) (2.6 kb)	12,000	20,558,110	38.650
cDNA	PacBio	Iso-Seq	Full transcripts (heart + testes) (2.0 kb)	10,000	18,985,944	29.496

Improvements to genome assembly completeness during scaffolding

Sequential steps of scaffolding, polishing, and quality control (Fig. 1, Supplementary Materials: Fig. S2, Table S3) improved the genome assembly statistics considerably from the initial SUPERNOVA *S. vulgaris* assembly (Supplementary Materials: Fig. S4). BUSCO completeness was approximately 94.6%, which was largely achieved by the initial assembly (92.9%), but somewhat improved over the additional assembly steps (Fig. 2a). The final BUSCO completeness score is comparable to other chromosome-level passerine assemblies on NCBI (Fig. 3a). BUSCO predictions are susceptible to base calling errors and can also fluctuate due to changes elsewhere in the genome assembly (Edwards 2019) (see section 2.8 BUSCO versus BUSCOMP performance benchmarking). As a consequence, BUSCO can under-report the true number of complete BUSCO genes in an assembly (Edwards et al., 2018; Field et al., 2020; Edwards et al., 2021). We therefore used BUSCOMP to compile complete BUSCO genes from across all stages of the assembly. Only 70 (1.4%) of the 4,915 Aves BUSCO genes were found to be "Missing" from all assembly versions, with 4,764 (96.9%) rated "Complete" in at least one stage (Fig 3a, BUSCOMP).

The final assembly had the fewest unmapped Iso-Seq reads (Fig. 2b), with the largest improvement seen post gap-filling, followed by chromosome scaffolding. An increase in missing Iso-Seq transcripts was observed after scaffolding with the Iso-Seq reads themselves,

and post long-read scaffolding, due to reads no longer partially matching at scaffold ends. Polishing caused a minimal improvement on the total number of mapped Iso-Seq reads, and none were lost during scaffold clean-up with DIPLOIDOCUS (runmode purgehaplotig and vecscreen). Assessment using GEMOMA and SAAGA revealed that across these assembly steps we see a generally consistent increase in the quality of the predicted proteins during annotation (Fig. 2c), with the largest increases occurring post long-read scaffolding, followed by chromosome scaffolding, and then scaffold clean-up.

Of the 33,454 high quality isoform transcripts in the PacBio Iso-Seq data, only 241 failed to map to the final genome assembly, a 17.2% decrease compared to the 291 that failed to map to *S. vulgaris* vNA (Fig. 3b).

Final genome assembly size, heterozygosity, and contiguity

The *S. vulgaris* vAU assembly of 1,049,838,585 bp covers approximately 93.78% of the total estimated 1.119 Gb genome size (Supplementary Materials: Appendix 2 Validation of SUPERNOVA genome size prediction using JELLYFISH). A similar estimation of genome completeness was reported by K-MER ANALYSIS TOOLKIT (KAT), with the raw read1s (forward reads) estimating a genome completeness of 96.7% (estimated genome size 1.125 Gb, estimated heterozygosity rate 0.57%) and read2s (reverse reads) estimating a genome completeness of 95.92% (estimated genome size 1.135 Gb, estimated heterozygosity rate 0.54%) (Supplementary Materials: Fig. S5). Predicted genome sizes based on either read1s or read2s using KAT were slightly larger than the estimation generated by JELLYFISH using all the read data, however the length range was relatively consistent (1.119-1.135 Gb). This assembly reports a scaffold N50 of 72.5 Mb and L50 of 5, with a total of 1,628 scaffolds (Table 2); 98.6% (1,035,260,756 bp) of the sequence length has been assigned to the 32 putative nuclear chromosomes (identified via the *T. guttata* v3.2.4 assembly), plus a mitochondrial genome. The final assembly contains 14 macrochromosomes (> 20 Mb, as

447 described in Backström et al., 2010), with relative sizes appearing in consensus with known
448 karyotype of *S. vulgaris* (Calafati & Capanna 1981). Macrochromosome scaffolds account
449 for 81.9% of the total assembly size, with the remainder on microchromosomes (16.9%) or
450 unplaced scaffolds. While these large scaffolds remain only putative chromosomes assuming
451 karyotype orthology until they can be validated with further read data, increased
452 completeness scores post chromosomal alignment across all assembly assessment metrics
453 (Fig. 2) support the assembly structure.

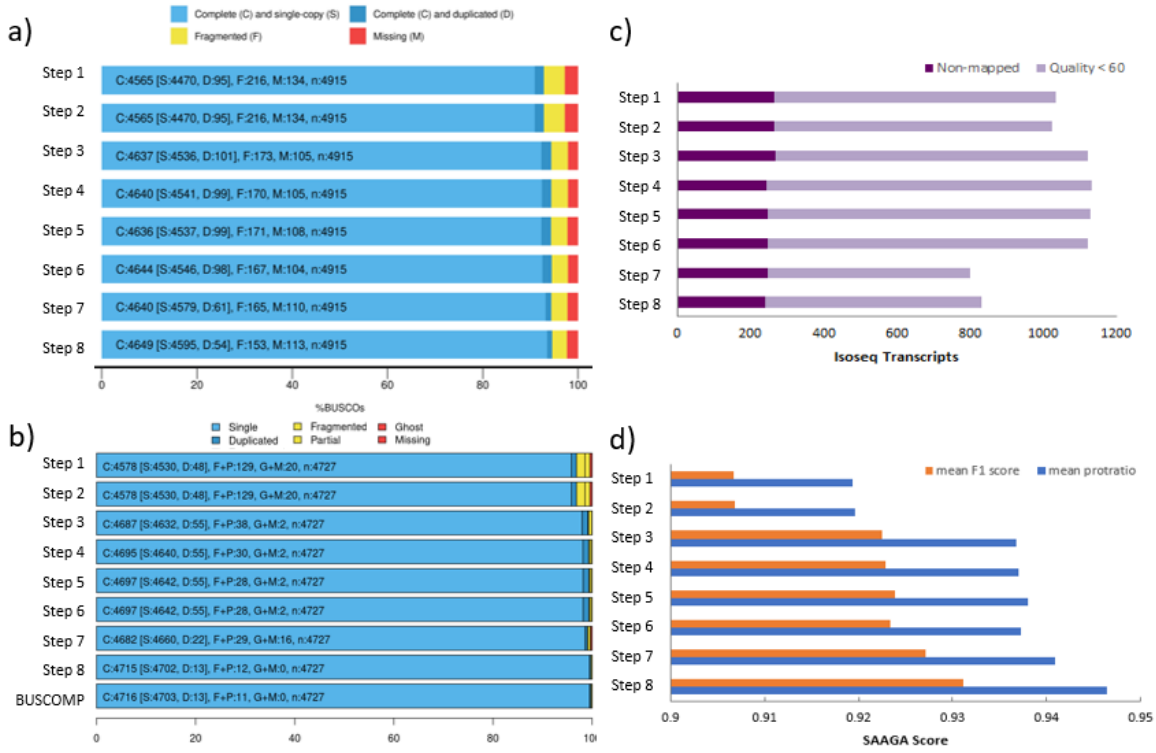

454

455 **Figure 2: *Sturnus vulgaris* vAU assembly steps overview.** Quality and completeness
456 assessments for eight sequential assembly steps: step 1 (SUPERNOVA assembly), step 2
457 (DIPLODOCUS primary assembly), step 3 (SSPACE-LONGREADS scaffolding), step 4
458 (GAPFINISHER gapfilling), step 5 (L_RNA_SCAFFOLDER), step 6 (PILON polishing), step 7
459 (DIPLODOCUS clean up), and step 8 (SATSUMA2 Chromosome scaffolding). **a)** BUSCO (Aves,
460 n=4,915) completeness rating summaries for the sequential steps of *S. vulgaris* genome
461 assembly. **b)** BUSCOMP completeness results for the 4,727 BUSCO genes identified as
462 single copy and complete in one or more assembly stages. The final BUSCOMP row
463 compiles the best rating for each gene across all eight steps. **c)** The number of Iso-Seq reads
464 that failed to map to each assembly step. **d)** SAAGA annotation scores of mean protein length
465 ratio (blue) and F1 score (orange) (see Methods for details).
466

Table 2: *Sturnus vulgaris* overview of assembly statistics for vAU1.0, vAU1.1, and vNA, assessed using BUSCOMP.

	***Sturnus vulgaris* vAU1.0**	***Sturnus vulgaris* vAU1.1**	***Sturnus vulgaris* vNA**
Total length (bp)	1,049,838,585	1,043,825,671	1,036,755,994
Number of scaffolds	1,628	1,344	2,361
Scaffold N50 (bp)	72,525,610	72,244,370	3,416,708
Scaffold L50	5	5	89
Largest scaffold (bp)	151,927,750	151,503,485	11,828,398
Mean scaffold length (bp)	644,864.0	776,656.01	439,117.3
Median scaffold length (bp)	1,337	1,343	4,856
Number of Contigs	23,815	23,340	22,666
Contig N50 (bp)	145,864	147,322	147,183
Contig L50	2,030	2,010	1,908
Gap (N) length (bp)	13,242,113 (1.26%)	0.74%	23,939,528 (2.31%)
GC (Guanine-Cytosine) content (%)	41.73%	41.72%	41.49%

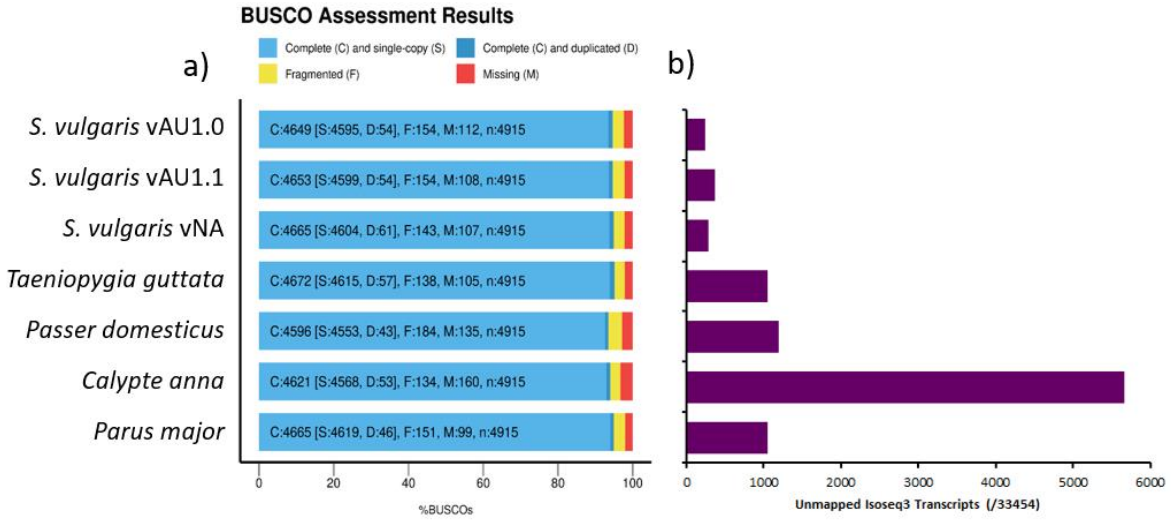

Figure 3: Assessment of *Sturnus vulgaris* and comparison avian reference assemblies. a) BUSCO (Aves) assessments of assembly completeness of *S. vulgaris* vAU1.0, and the NCBI uploaded genome *S. vulgaris* vAU1.1, presented alongside *S. vulgaris* vNA and four recent high-quality avian reference genomes (*Taeniopygia guttata* assembly accession GCF_008822105.2, *Passer domesticus* assembly accession GCA_001700915.1, *Calypte anna* assembly accession GCA_003957555.2, *Parus major* assembly accession GCA_001522545.3). **b)** Total number of Iso-Seq transcripts that failed to map to each assembly.

3.2 *Sturnus vulgaris* vAU whole transcriptome data analysis

We generated approximately 68 Gb of PacBio Iso-Seq whole transcript (39,544,054 subreads) (Table 1). This produced a total of 33,454 clustered high-quality (predicted accuracy ≥ 0.99) reads, and 157 clustered low-quality (predicted accuracy < 0.99) reads (Supplementary Materials: Table S4). These high-quality read data were used to improve the scaffold assembly of the genome using L_RNA_SCAFFOLDER (see section 2.1) and assess genome completeness (using count comparison of unmapped Iso-Seq reads, see section 2.5.2). After being passed through the TAMA *collapse* pipeline, a total of 28,448 non-redundant transcripts were retained to create the final *S. vulgaris* vAU transcriptome, which was used for gene prediction when completing the annotation of the genome assembly. This final three tissue (brain, gonad, heart) Iso-Seq transcriptome had a moderate level overall BUSCO completeness of around 63% that compares to other avian Iso-Seq transcriptomes (Fig. 4a), with a wide range of gene ontology terms identified in the final Iso-Seq transcript list (Fig. 4b) that resembled other avian Iso-Seq GO term distributions (Yin et al., 2019).

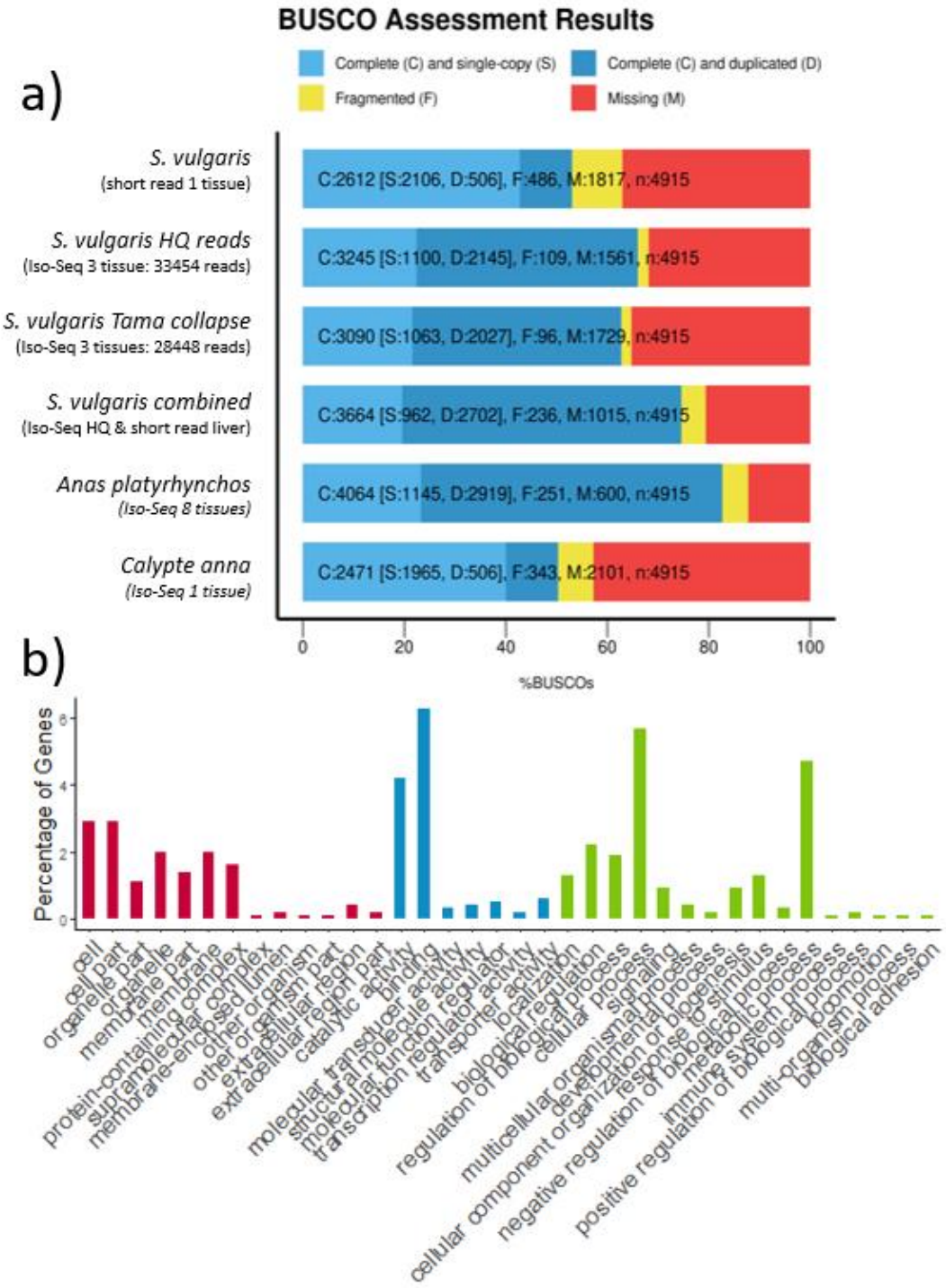

Figure 4: Assessment of 3 tissue Iso-Seq (brain, gonad, heart) *Sturnus vulgaris* transcriptome. a) BUSCO (aves) rating summaries for *S. vulgaris* short read liver transcriptome, the high quality Iso-Seq *S. vulgaris* transcript produced though the Iso-Seq v3.3 pipeline, the final *S. vulgaris* transcriptome produced by TAMA *collapse* pipeline, and combined high quality Iso-Seq and short read liver transcripts, alongside two other avian Iso-Seq transcriptomes (*Anas platyrhynchos* using pectoralis, heart, uterus, ovary, testis, hypothalamus, pituitary and 13 days-old embryo tissue (Yin et al., 2019), and *Calypte anna* using liver tissue (Workman et al., 2018)). **b)** Breakdown of major GO terms in the sequenced Iso-Seq reads, with Cellular Component (red) Molecular Function (blue) and Biological Process (green).

3.3 *Sturnus vulgaris* genome annotation

The initial annotation produced by GeMoMa, informed by the 26 avian genome annotations available at the time on Ensembl (Supplementary Materials, Table S1), predicted 21,539 protein coding genes, with 97.2% BUSCO completeness (93.1% complete when longest protein-per-gene extracted with SAAGA) (Fig. 5). The initial Maker2 annotation reported 13,495 genes, and a BUSCO completeness of 79.5% (Fig. 5). The merged final annotation reported a BUSCO completeness of 98.2% (Fig. 5a), and this annotation predicted a total of 21,863 protein-coding genes and 79,359 mRNAs. There was an average of 10.7 exons and 9.7 introns per mRNA, with an average intron length of 3,364 (Table 3). Of these, 1,764 are single-exon genes and 2,330 single-exon mRNA. Predicted coding sequences make up 5.4% of the assembly, with 44.77% remaining outside any gene annotation (Fig. 5b).

The predicted transcripts were mapped using SAAGA to the Swiss-Prot database, with 66,890 transcripts returning successful hits (84.3%) and 12,469 transcripts remaining unknown (15.7%) for the final annotation (Fig. 6a). The known proteins had an average length of 652 amino acids (aa) and the unknown proteins had an average length of 426 aa (Fig. 6a). Most of the predicted proteins were of high quality, with around 56% of them having an F1 score (see Methods) of greater than 0.95 (Fig. 6b). Similar results were seen when the *Gallus gallus* reference proteome was used, with 69,714 known proteins of average length of 646 aa, and 9,645 known proteins of average length of 401 aa, and the final merged annotation having the same F1 score distribution (Fig 6c & 6d).

The GeMoMa annotation had similar protein quality patterns, with 57,026 known proteins (average length 664 aa), and 10,400 unknown proteins (average length 401 aa) (Fig. 6e). The Maker2 displayed much greater similarity in protein length histogram between known and unknown proteins, with shorter proteins with known homologs (average length 565 aa), but longer unknown proteins (average length 549 aa) (Fig. 6f). The *S. vulgaris* vNA

annotation final merged annotation had extremely similar statistics to the final *S. vulgaris* vAU annotation, with an average known protein length of 650 aa, and an average unknown protein length of 407 aa (Supplementary Materials: Figure S2b).

3.4 *Sturnus vulgaris* genome-wide patterns of genomics features

Transcript density compared between mapped Iso-Seq reads and predicted transcripts in the final annotation displayed similar patterns, with some minor variation in patterns between the two tracks (Fig. 7; track 1). Final predicted gene densities (Fig. 7; track 2) were largely following the patterns seen in transcript densities. Further, patterns of transcript and gene numbers across the genome track relatively consistently to GC content (Fig. 7; track 4).

Global whole genome variant data (Fig. 7; track 3) revealed genomic regions where variant density is low or non-existent, indicative of high genetic conservation across the species, and genomic regions where variant density peaks are indicative of variant hotspots. Interestingly, we see regions of high conservation corresponding to peaks in gene and/or transcript numbers (e.g., midway through chromosome 4), which may be indicative of regions of highly conserved genes and possibly centromere locations.

Table 3: Summary of genome annotation of *Sturnus vulgaris* vAU and vNA assemblies. Statistics extracted using AGAT *agat_sp_functional_statistics.pl*.

Genome Annotation		*S. vulgaris* vAU	*S. vulgaris* vNA
Genes	**Total number**	21,863	21,944
	Average length	34,699 bp	35,761 bp
	mean mRNAs per gene	3.6	3.7
mRNA	**Total number**	79,359	81,714
	Average length	38,073 bp	37,857 bp
	mean exons per mRNA	11.8	11.8
CDS	**Total number**	79,359	81,714
	Average length	1,851	1,836
	Average intron in CDS length	3,364	3,343
Exons	**Total number**	933,014	962,220
	Mean length	163	158
Gene Function	**Ontology Term**	60.26% (13174/21863)	59.68% (13097/21944)
	InterPro	78.87% (17244/21863)	77.57% (17022/21944)
	SUPERFAMILY	60.36% (13197/21863)	58.26% (12786/21944)

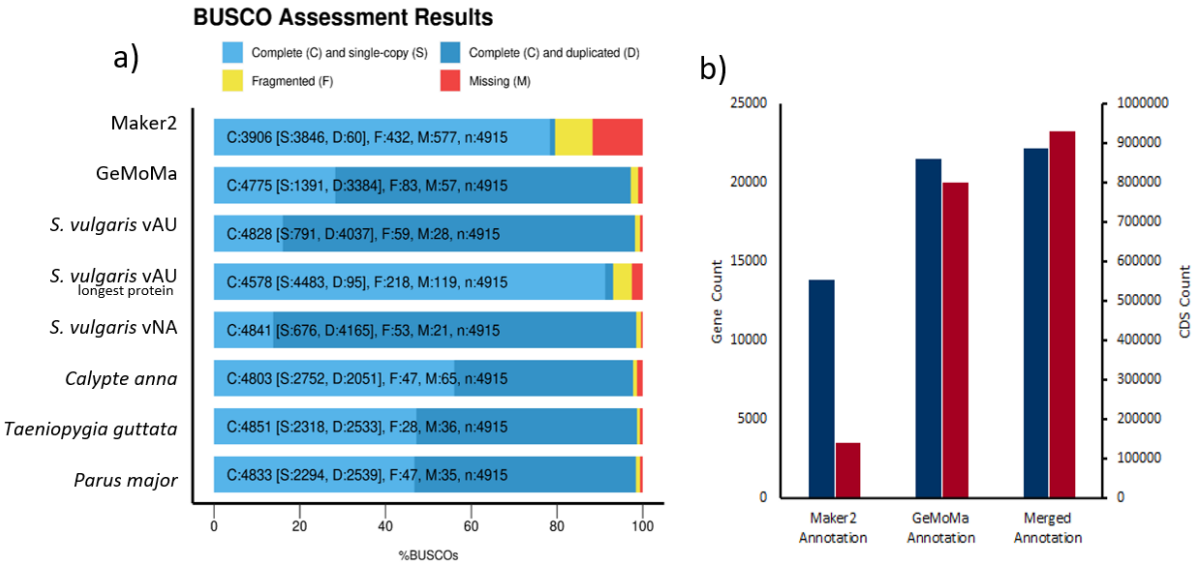

Figure 5: *Sturnus vulgaris* assessment of annotation. a) BUSCO (Aves) assessments of initial MAKER2 and GEMOMA assemblies, the final *S. vulgaris* vAU annotation, the final annotation with the longest protein-per-gene extracted using SAAGA, the final *S. vulgaris* vNA annotation (combined GEMOMA and MAKER2 annotation), and the ensemble annotations of three additional passerines. **b)** The number of genes (blue) and CDS (red) in the MAKER2 annotation, GEMOMA annotation, and merged annotation.

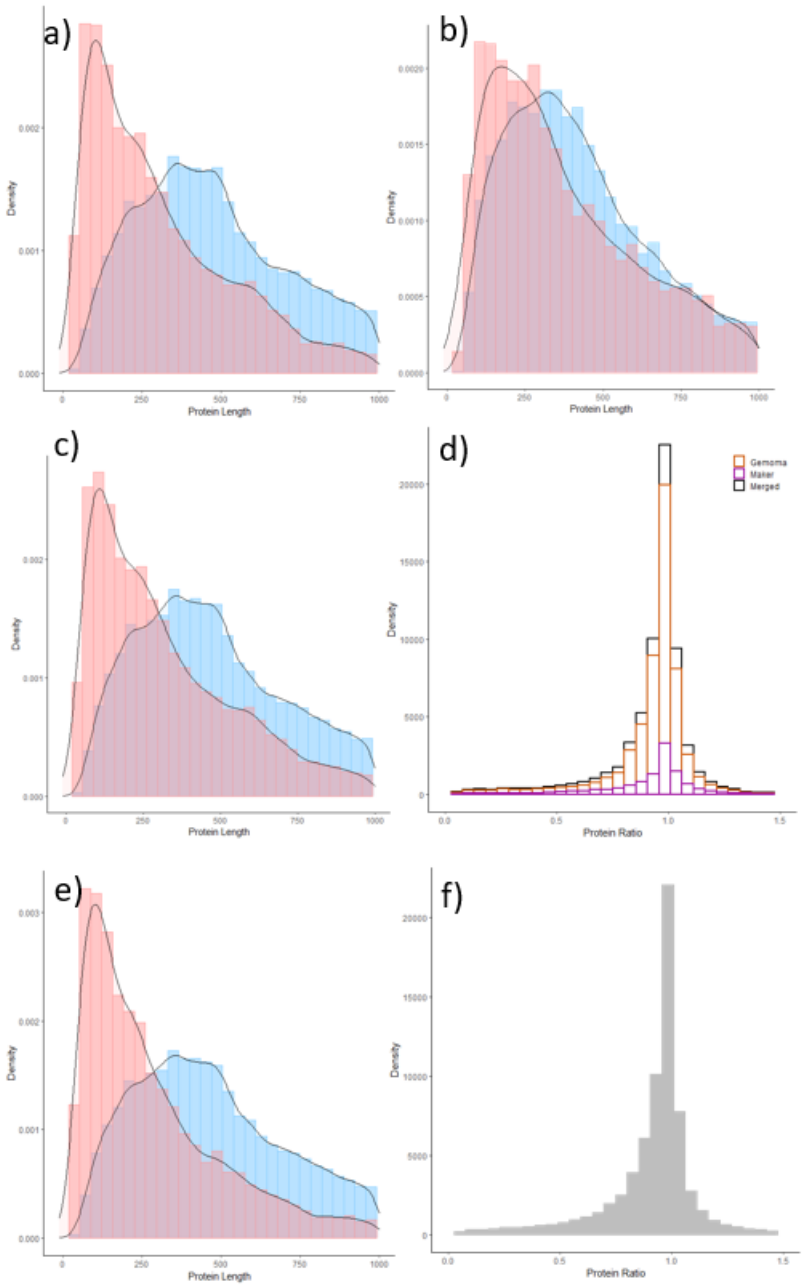

Figure 6: Summary of predicted annotated proteins. a) Protein lengths for known proteins (blue, with a located Swiss-Prot comparison) and unknown proteins (red, those that did not map to Swiss-Prot) for the GeMoMa annotation compared to Swiss-Prot. **b)** Protein lengths of known and unknown proteins for the Maker2 annotation compared to Swiss-Prot. **c)** Protein lengths of known and unknown proteins for the merged GeMoMa and Maker2 annotation compared to Swiss-Prot. **d)** Protein length ratio between output from SAAGA for all known Swiss-Prot proteins (where a score close to 1 indicates a high-quality gene annotation, protein length ratio calculated as annotated protein length / best Swiss-Prot reference protein length) (merged annotation = black, GeMoMa annotation = orange, Marker2 annotation = purple). **e)** Protein lengths of known and unknown proteins for the merged GeMoMa and Maker2 annotation compared to *Gallus gallus* reference proteome (UP000000539_9031). **f)** Protein length ratio between output from SAAGA for the merged annotation against the *Gallus gallus* reference proteome.

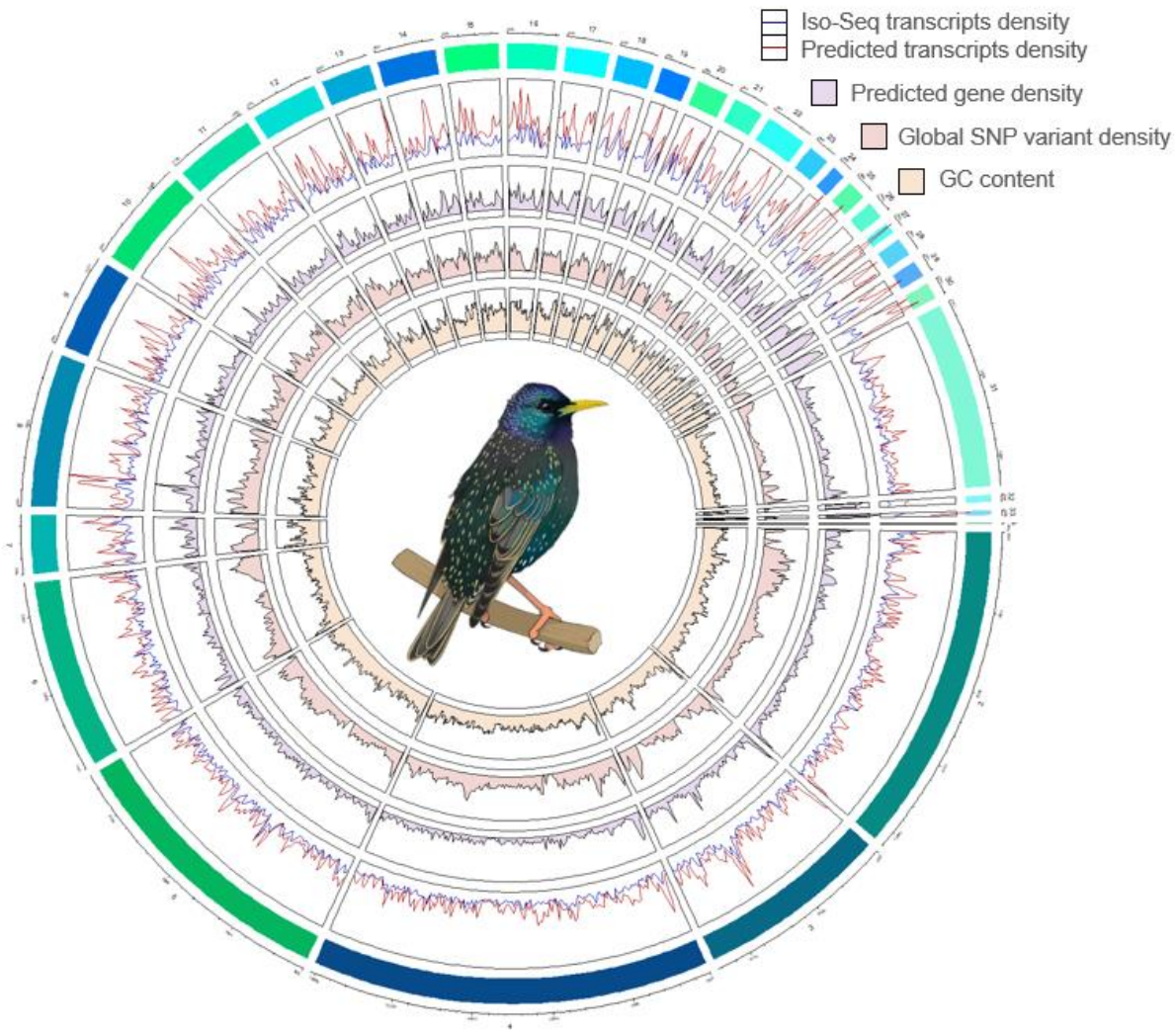

Figure 7: CIRCLIZE plot of the 33 main chromosomal scaffolds (32 putative autosomes plus mtDNA) in the Sturnus vulgaris (*S. vulgaris* vAU) genome assembly (>98% of the total assembly length). The tracks denote variable values in 1,000,000 bp sliding windows. From the outermost track in, the variables displayed are track 1 (Iso-Seq transcripts as blue line, final annotation transcripts as red line), track 2 (final annotation gene counts, purple area), track 3 (variant density, red area), and track 4 GC content (yellow area).

3.5 BUSCO versus BUSCOMP performance benchmarking

For the non-redundant pseudodiploid *S. vulgaris* vAU SUPERNOVA assembly, BUSCOMP revealed differences in the BUSCO ratings of scaffolds dependent on the assembly background (Fig. 8). Despite the primary ('pri') assembly being a subset of the non-redundant pseudodiploid ('dinpnr') assembly, it identified more "Complete" BUSCO genes (4,565 versus 4,532) with fewer "Missing" (131 versus 171) (Fig. 8a). The alternative assembly ('alt') subset similarly returned a partially overlapping set of BUSCO genes with 'dipnr', including some not found in 'dipnr' or 'pri': in total, only 101 genes were missing from all three assemblies. Reducing the primary assembly to the 968 (of 18,439) scaffolds containing a complete BUSCO gene ('pribusco'), increased the number of complete genes from 4,565 to 4,586 and reduced the number missing from 131 to 112. Most unexpectedly, reverse complementing these scaffolds reduced the complete BUSCO by two genes and increased the number missing by fifteen (Fig. 8a). All five assemblies returned complete BUSCO genes that were fragmented or missing in all the other four assemblies (Supplementary File 1, BUSCOMP v3 results), for a combined total of 4,760 complete and only 74 missing.

Adding direct or reverse-complemented copies of the 'pribusco' scaffolds increased the number of "Duplicated" genes, but still returned single copy complete genes (Fig. 8b). Doubling and then tripling the assembly size also increased the number of "Missing" genes from 112 to 198 ('duplicate') and then 207 ('triplicate'). As before, these summary numbers hide some gene gains as well as gene losses; only 77 genes are missing from all three BUSCO runs, with 4,750 returned as complete by at least one. Adding randomly shuffled versions of the 'pribusco' scaffolds only had a marginal effect on BUSCO ratings, with four ('2n') to five ('3n', '4n') fewer complete genes returned and seven additional genes missing

following addition of the random sequences (Fig. 8c). Ten replicate analyses of the `pribusco` scaffolds returned identical results (Supplementary File 1, BUSCOMP v3 results).

In contrast, BUSCOMP completeness is much more consistent across all datasets, with the primary assembly returning the same numbers of complete, partial/fragmented and missing genes as the pseudodiploid assembly (Supplementary File 1, BUSCOMP v3 results). Similarly, reverse complementing scaffolds or increasing genome size gives no difference to the completion statistics. Unlike BUSCO, BUSCOMP rates 100% of complete BUSCO genes for duplicated or triplicated scaffolds as ‘Duplicate’ rather than ‘Single Copy’. Most reassuringly, every complete BUSCO gene returned by a variant or subset of the pseudodiploid assembly is also returned as ‘Complete’ in the pseudodiploid assembly itself. Results using BUSCO v5 and the updated lineage data were qualitatively the same as v3, showing largely identical trends (Supplementary File 2, BUSCOMP v5 results). The exception is that reverse-complementing scaffolds reduced the complete BUSCO genes by one (7,555 to 7,554) and increased the number missing by one (391 to 392). Curiously, this was not reflected by analysis of the duplicated scaffolds, in which all 7,555 ‘pribusco’ complete genes were returned as complete and duplicated. It should be noted that the ‘pribusco’ scaffolds for the v5 analysis are missing a greater proportion of the BUSCOMP-compiled single copy complete BUSCO genes because they were still defined from v3 data.

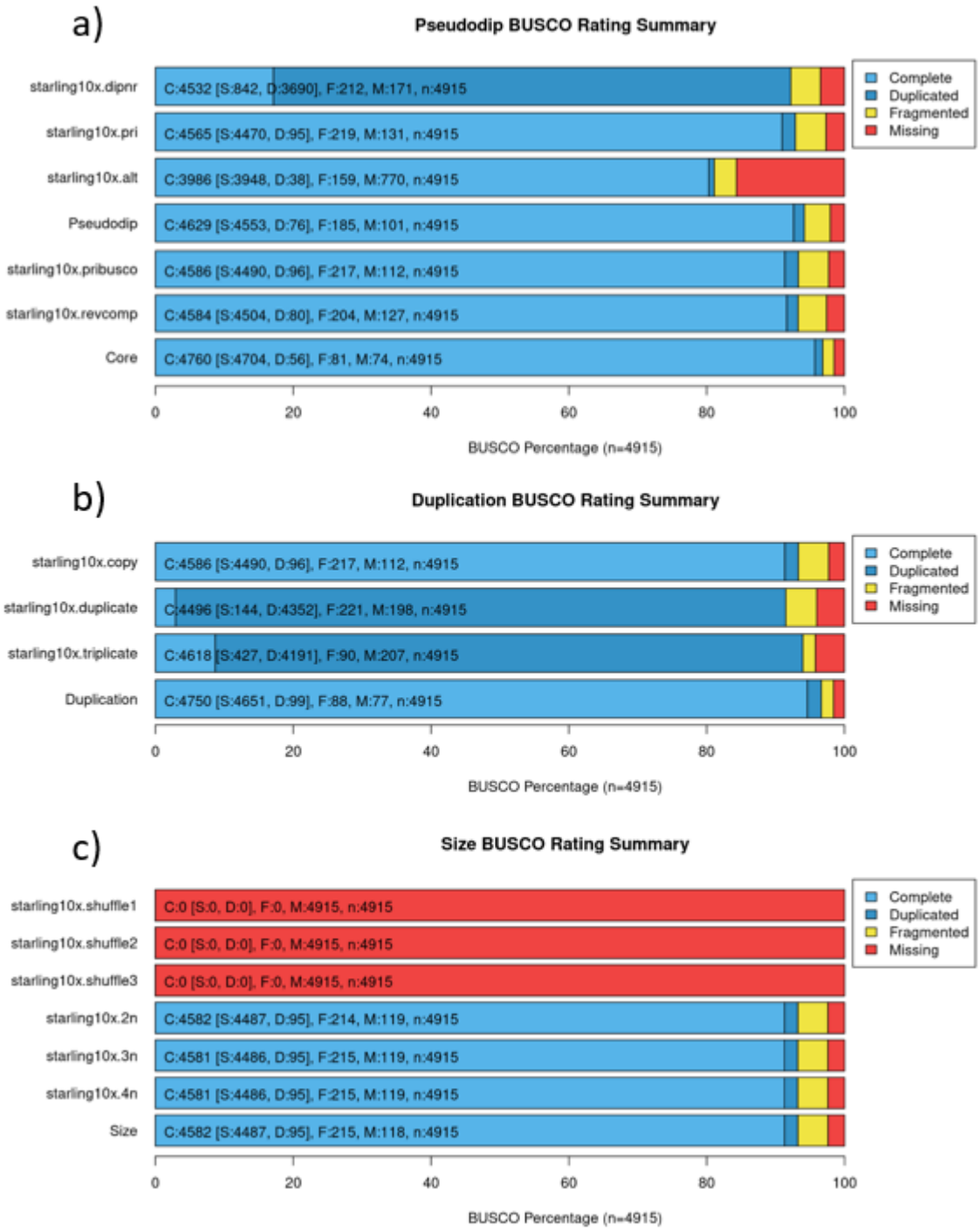

Figure 8. Compiled BUSCO results for benchmarking data.

4. Discussion

Here, we present a high-quality, near-complete reference genome for the European starling, *Sturnus vulgaris* vAU, with chromosome-level scaffolding that assigns 98.6% of the genome assembly length to 32 putative nuclear chromosome scaffolds. We demonstrate the utility of both transcripts and gene annotation in validating *S. vulgaris* vAU assembly processes. BUSCOMP, Iso-Seq transcript, and SAAGA annotation assessment were largely in agreement with one another, though each provided additional fine-scale feedback on assembly improvements achieved by each assembly step. These analyses highlight the benefits of these complementary assessment approaches in ensuring that aspects of genome quality are not sacrificed to improve non-specific assembly quality metrics, such as N50. We also present a second, North American, genome assembly, *S. vulgaris* vNA (GCF_001447265.1). Overall, the *S. vulgaris* vAU assembly improved genome assembly statistics over the *S. vulgaris* vNA genome, with a greater percentage of the estimated 1.119 Gb genome represented (94% vs 93%), an increase of scaffold N50 from 3.42 Mb to 72.5 Mb, and a decrease in scaffold L50 from 89 to 5. The *S. vulgaris* vNA still has good assembly statistics (Table 2, Table S3) and has a marginally higher BUSCO completeness (Fig. 3a) and BUSCOMP completeness (Supplementary Materials: Fig. S6) of approximately 20 BUSCO sequences. There is increasing recognition of the importance of pan-genomes (genome assemblies that differentiate between genes/regions shared by all members of the species, and dispensable or rare genes/regions) (Hirsch et al., 2014; Sherman & Salzberg 2020), which are essential for many model organisms (Vernikos et al., 2015). Having these two high-quality *de novo* assemblies from different populations will improve future genomic work on the global invasive populations of this species, and facilitate review of structural variation (e.g., inversions) that may exist across different populations. It should be noted, however, that the final scaffolding step for *S. vulgaris* vAU assumed structural conservation

687 between the starling and zebra finch and thus future synteny analyses may want to use the
688 earlier assembly step.

689 **4.1 BUSCO and BUSCOMP assembly completeness assessment**

690 BUSCO (Simão et al., 2015) is an extremely useful and widely-used used assembly
691 assessment tool, providing information on which conserved lineage specific genes are
692 present, fragmented, or absent from a genome assembly. The program, however, can suffer
693 from inconsistent BUSCO gene identification, where a particularly BUSCO may be dropped
694 from a report due to changes to contigs or scaffolds elsewhere in the assembly (Edwards
695 2019), which can result in under-reporting of assembly completeness (Edwards et al., 2018;
696 Field et al., 2020; Edwards et al., 2021). Here, we confirm this behaviour on benchmarking
697 datasets derived from the *S. vulgaris* vAU pseudodiploid 10x linked read assembly
698 (Supplementary Materials: Fig. S3, 8). Adding and removing scaffolds can both alter the
699 BUSCO ratings for "Complete" genes within the unchanged scaffolds (Fig. 8, Supplementary
700 File 1, BUSCOMP v3 results, Supplementary File 2, BUSCOMP v5 results). Many of these
701 changes are likely to be the consequence of changes in score thresholds and/or gene
702 prediction models. However, we also demonstrate some unexpected behaviours that are
703 harder to explain, such as changes to BUSCO gene ratings when scaffolds are reverse
704 complemented (Fig 8a).

705 This unpredictable variability in the identification of BUSCOs across genome
706 assembly versions poses some obvious challenges when trying to compare alternate versions
707 of the same assembly. This is particularly true when trying to interpret small changes in
708 BUSCO ratings as assemblies near completion. In addition, an important feature of BUSCO
709 is that it incorporates sequence quality in the context of the gene prediction models it
710 generates. This is desirable for assessing final assembly quality, but can present problems
711 when comparing early assembly stages, prior to error-correction by "polishing". BUSCOMP

712 (https://github.com/slimsuite/buscomp) is robust to differences in assembly size and base-
713 calling quality and rates the "completeness potential" of an assembly based on the presence
714 of genes first identified for that species by BUSCO. Here, we used BUSCOMP analysis of
715 sequential assembly steps to gain a more accurate understanding of how assembly decisions
716 affected genome completeness (Fig. 2, Supplementary Materials: Fig. S4). BUSCOMP
717 analysis can then be complemented by other tools, such as KAT (Mapleson et al., 2017),
718 SAAGA (https://github.com/slimsuite/saaga), and BUSCO itself to get additional assessment
719 of sequence quality.

720 **4.1. Transcript- and annotation-guided *Sturnus vulgaris* vAU genome assembly**

721 The assembly of the *S. vulgaris* vAU genome was improved by assessing mapped Iso-
722 Seq whole transcripts and quality scores of predicted proteins from homology-based
723 annotation. Mapping of the high quality Iso-Seq reads proved to be an extremely fast method
724 of assessment (33,454 Iso-seq sequences mapped in <5 mins with 16 CPU cores), while the
725 GeMoMa and SAAGA compute time of 12 hrs per assembly was roughly comparable to
726 BUSCO (approximately 50 CPU hrs per assembly on an average machine), though more
727 computationally intensive (GeMoMa ran for approximately 200 CPU hours per assembly,
728 and SAAGA ran for approximately 8 CPU hours per assembly). Over the eight sequential
729 assembly steps, there was a decrease in unmapped Iso-Seq reads, indicating improved
730 sequence representation, primarily due to gap-filling yielding the greatest decrease in
731 unmapped Iso-Seq transcripts across all assembly steps. Similarly, the quality of annotated
732 proteins predicted by GeMoMa, as assessed by SAAGA, demonstrated ongoing
733 improvements through ONT scaffolding, clean-up, and chromosome alignment. It is also
734 noteworthy that increases in large-scale sequence connectivity using the *T. guttata* genome
735 (Peona et al., 2018) improved the assembly's performance across all metrics, including

736 completeness estimates, although future Hi-C (or similar) analysis will be required to confirm
737 the predicted genome structure.

738 Further, BUSCOMP provided an important means of standardising BUSCO
739 annotation ratings across the multiple assembly steps. This method, together with the mapped
740 Iso-Seq reads, can deal with the unpolished intermediary genome steps, and does not suffer
741 the same sequence identification accuracy issues as the traditional stand-alone BUSCO
742 analysis. Together, the standardised assessment reported by BUSCOMP, and the
743 comprehensive and genome/species specific set of genes provided by Iso-seq and
744 GEMOMA/SAAGA showcase the complementary features of these annotation approaches for
745 assembly assessment.

746 **4.2. Improvements to contiguity and completeness during *Sturnus vulgaris* vAU genome**
747 **assembly**

748 Several alternative assembly pipelines were assessed (Supplementary Materials: Fig.
749 S2) and most of the upstream assembly decisions were based primarily on establishing
750 reasonable base assembly statistics (scaffold N50, scaffold L50, contig numbers). Assembly
751 size increased during scaffolding steps, due to estimated bases in gaps, while a decrease in
752 assembly size was only seen during scaffold clean up using *Purgehaplotigs*. Of all the
753 scaffolding steps, scaffolding with the low coverage ONT long reads resulted in the greatest
754 decrease of scaffold L50 (146 scaffold to 39 scaffold, Supplementary Materials: Fig. S4d)
755 and total scaffold number (18,439 scaffolds to 7,856 scaffolds, Supplementary Materials: Fig.
756 S4a). It has previously been shown that even low coverage of ONT data in conjunction with
757 10x may produce high quality genome assemblies (Ma et al., 2019). This was true for our
758 data, which demonstrates the utility of even low coverage, long read sequencing
759 (approximately 4.5% coverage based on the estimated genome size of 1.119 Gb) in greatly
760 improving the contiguity of scaffolds generated by short read genome assemblers (though Hi-

C data may serve this purpose at a lower cost to scaffold ratio and may assist in identifying misassemblies, which is often not a focus of long-read scaffolding tools). While additional scaffolding using the Iso-Seq whole transcripts did not result in a large increase in continuity (Supplementary Materials: Fig. S4), the Iso-Seq reads were nevertheless were able to scaffold some sequences that failed low coverage ONT scaffolding, reducing the total scaffold count by approximately 100 (7,856 scaffold to 7,776 scaffolds, Supplementary Materials: Fig. S4a). This long-read transcript scaffolding served to minimise the number of fragmented genes in the final assembly, helping downstream analysis and gene prediction models. The final assembly maintained reasonably short contig N50 and high contig L50, which will only be improved with much more extensive long-read sequencing of the species. Nevertheless, scaffolding the *S. vulgaris* genome against that of *T. guttata* was able to further scaffold the genome to a predicted chromosome level, assigning 98.6% of the assembly to previously characterised chromosomes. In support of the assumed synteny of this step, we saw small increases in assembly quality and completeness metrics.

The final two assembly steps (contig clean up and chromosomal alignment) were primarily guided by high BUSCO scores and low missing Iso-Seq transcripts (Supplementary Materials: Figure S3). DIPLOIDOCUS *vecscreen* did not flag any contamination and so did not result in any assembly decreases. Over-pruning of contigs during clean up (using DIPLOIDOCUS *DipCycle* which is stricter than just *Purgehaplotigs*) resulted in too many (>1,000) discarded scaffolds that decreased assembly completeness scores, most likely because of low coverage ONT long read data. While this drastically improved assembly statistics, this came at the cost of dropped BUSCO sequences. Lastly, assembly duplication analysis using KAT agreed with BUSCO results, indicating there was little final assembly sequence duplication when comparing to raw read k-mer counts (Supplementary Materials: Fig. S5).

4.3. *Sturnus vulgaris* vAU transcriptome

When comparing the completeness of this new starling transcriptome data to existing Illumina short read transcript data produced using liver tissue (Richardson et al., 2017), we see an increase of about 20% in BUSCO completeness, with a particularly large increase in the number of duplicated BUSCO, a result of the alternate transcript isoforms captured through the Iso-Seq. Assessing the effect the TAMA pipeline had on BUSCO completeness, we see a small drop in complete BUSCOs (Fig. 2a) that appear to have been lost during the mapping to genome assembly step. Finally, comparing our final transcriptome to two other avian Iso-Seq transcriptomes gives an indication of how much unique transcript information is added by the addition of tissues into pooled Iso-Seq sequencing runs. The single tissue Iso-Seq liver transcriptome of *Calypte anna* (Anna's hummingbird) (Workman et al., 2018) reported similar BUSCO completeness to the short read *S. vulgaris* liver transcriptome. The eight tissue Iso-Seq transcriptome of *Anas platyrhynchos* (mallard) (Yin et al., 2019) yielded an increase of 30% in complete BUSCOs, consistent with the expectation that our three-tissue Iso-Seq library will be missing a number of tissue-specific genes.

4.4. *Sturnus vulgaris* genome annotation

Of the approximately 22,000 genes reported in the final annotation, 65% were from GEMOMA, and 35% from MAKER2, with the source being randomly selected for common annotation. MAKER2 predicted a higher number of genes in *S. vulgaris* vNA versus *S. vulgaris* vAU (15,150 vs 13,495), while GEMOMA predicted a higher number of genes in the *S. vulgaris* vAU genome (21,539 vs 20,414). The ratio in predicted MAKER2 and GEMOMA was more biased towards the homology-based predictor, with an approximate ratio of 1:5 between MAKER2 and GEMOMA (Fig. 5b). Merging of the MAKER2 annotation to the GEMOMA annotation resulted in an increase in 1.1.% in BUSCO completeness. Duplication levels were much higher in the GEMOMA annotation when compared to MAKER2 (Fig. 5a).

This is not unreasonable, as the GeMoMa annotation will be biased toward well-characterised genes and so may contain more transcripts per gene (Fig. 5b), whereas Maker2 will inform the prediction of more taxon or possibly species-specific coding sequences. High congruence between Iso-Seq and predicted transcript numbers indicate regions of accurate annotation predictions (Fig. 7). In contrast, Iso-Seq transcripts that are dissimilar or much lower to the predicted transcript densities, are either genomics regions producing tissue specific transcripts not captured by their brain, testes, or muscle, or more likely annotated transcript overprediction.

For the final *S. vulgaris* vAU annotation, the predicted proteins of unknown origin (those that failed to map to Swiss-Prot database or *Gallus gallus* proteome) had a smaller average length than those with known homologs (Fig. 6a & 6c). Similar results were found when this approach was used to assess genes predicted in the *R. marina* genome assembly (Edwards et al., 2018), and are indicative that these 'unknown' proteins are fragmented and lower quality predictions that may be due to underlying assembly issues with contiguity or frameshifting indels. The poorer quality could also reflect low stringency Maker2 gene predictions or homology based GeMoMa annotation of low-quality reference genes. The known proteins predicted by Maker2 (Fig. 6f) were of apparent lower quality than those reported by GeMoMa as indicated by their shorter lengths and lower protein ratios (Fig. 6e), which may be a result from a combination of incorrect gene predictions, and the high-quality reference homologs inflating quality scores of the GeMoMa annotation in comparison. The known protein lengths were similar across the *S. vulgaris* vAU and vNA annotations (652 vs 650 aa), though there was a slightly larger difference in average unknown protein length (426 vs 407 aa). Although this increase in *S. vulgaris* vAU is very slight, it may indicate increased quality of unknown protein predictions in the vAU annotation, possibly due to the more Iso-Seq data mapping to the vAU genome (Fig. 4b) or the higher contiguity.

Predicted genes were more commonly shorter than their closest reference protein hits, indicative there might still be some truncated gene predictions, consistent with the large number of assembly gaps. Nevertheless, the final annotation has a strong protein ratio peak around 1.0 for known proteins (Fig. 6b & 6d), indicating that the bulk of these predicted genes were of lengths similar to their Swiss-Prot homologs and hence deemed high quality.

Near identical assembly pipelines were used for the annotation of the two genome assemblies, with the resulting final gene count predictions comparable to other high-quality avian genomes and expected gene counts in eukaryote genomes. Both genome assembly versions reported similar final annotation statistics, with *S. vulgaris* vNA reporting slightly more predicted genes (Table 3), and a larger predicted gene coverage over the genome (59.09% gene coverage vs 55.23%), indicating this increase in predicted genes is not just a result of more overlapped predictions, though it could be a result of smaller assembly size and higher gene duplication (Fig. 5a).

5. Conclusion:

This paper highlights the multifunctional use of species-specific transcript data, and the importance of diverse assessment tools in the assembly and assessment of reference genomes and annotations. We present a high-quality, annotated *S. vulgaris* vAU reference genome, scaffolded at the chromosome level. Alongside a second assembly, *S. vulgaris* vNA, these data provide vital resources for characterising the diverse and changing genomic landscape of this globally important avian. In addition to improving the completeness of gene annotation, we demonstrate the utility of long-read transcript data for genome quality assessment and assembly scaffolding. We also reveal some counter-intuitive behaviour of BUSCO genome completeness statistics, and present complementary two tools, BUSCOMP

and SAAGA, which can identify and resolve potential artefacts, and inform assembly pipeline decisions.

Author Contributions

Project conception: all authors

Sample Collection: KCS, SJW, MCB

Lab Work: KCS, YC, LAR, WCW

Data Analysis: KCS, RJE, YC, WCW

Program Development: RJE

Manuscript Writing: KCS, RJE

Manuscript Editing: All authors

Acknowledgements:

We thank non-author members of the Starling Genome Consortium for their support of this project including Wim Vanden Berghe. Thank you to Stella Loke, Annabel Whibley, and Mark Richardson for their guidance of Nanopore sequencing and analysis. Thank you to Daniel Selechnik for assistance with RNA extractions. Art credit (Fig. 7 illustration) to Megan Bishop. RJE was funded by the Australian Research Council (LP160100610 and LP18010072). DWB and YC acknowledge grant funding from the Human Sciences Frontier Programme (Grant RGP0030/2015). SM acknowledges Roslin Institute Strategic Grant funding from the UK Biotechnology and Biological Sciences Research Council (BB/P013759/1). LAR was supported by a Scientia Fellowship from UNSW.

Programs

BUSCOMP documentation: https://slimsuite.github.io/buscomp/

Diploidocus documentation: https://slimsuite.github.io/diploidocus/

SAAGA documentation: https://slimsuite.github.io/saaga/

887 **References:**

888 Backström N, Forstmeier W, Schielzeth H, Mellenius H, Nam K, Bolund E, Webster MT, Öst T,
889 Schneider M, Kempenaers B *et al.* 2010 The recombination landscape of the zebra finch
890 Taeniopygia guttata genome. *Genome Research* **20** 485–495. (doi:10.1101/gr.101410.109)

891 Balakrishnan CN, Edwards SV & Clayton DF 2010 The Zebra Finch genome and avian genomics in the
892 wild. *Emu - Austral Ornithology* **110** 233–241. (doi:10.1071/MU09087)

893 Bateson M & Feenders G 2010 The use of passerine bird species in laboratory research: implications
894 of basic biology for husbandry and welfare. *ILAR Journal* **51** 394–408.
895 (doi:10.1093/ilar.51.4.394)

896 BirdLife International 2020 Species factsheet: Sturnus vulgaris. In *BirdLife International*.

897 Bodt LH, Rollins LA & Zichello J 2020 Genetic Diversity of the European Starling (Sturnus vulgaris)
898 Compared Across Three Invasive Ranges.

899 Boetzer M & Pirovano W 2014 SSPACE-LongRead: scaffolding bacterial draft genomes using long
900 read sequence information. *BMC Bioinformatics* **15** 211. (doi:10.1186/1471-2105-15-211)

901 Bomford M & Sinclair R 2002 Australian research on bird pests: impact, management and future
902 directions. *Emu - Austral Ornithology* **102** 29–45. (doi:10.1071/MU01028)

903 Bradnam KR, Fass JN, Alexandrov A, Baranay P, Bechner M, Birol I, Boisvert S, Chapman JA, Chapuis
904 G, Chikhi R *et al.* 2013 Assemblathon 2: evaluating de novo methods of genome assembly in
905 three vertebrate species. *GigaScience* **2**. (doi:10.1186/2047-217X-2-10)

906 Calafati P & Capanna E 1981 Karyotype analysis in ornithological studies: the chromosomes of six
907 species of oscines (passeriformes). *Avocetta* **5** 1–5.

908 Camacho C, Coulouris G, Avagyan V, Ma N, Papadopoulos J, Bealer K & Madden TL 2009 BLAST+:
909 architecture and applications. *BMC Bioinformatics* **10** 421. (doi:10.1186/1471-2105-10-421)

910 Coleman JD 1977 The foods and feeding of starlings in Canterbury. *Proceedings (New Zealand*
911 *Ecological Society)* **24** 94–109.

912 Davey NE, Shields DC & Edwards RJ 2006 SLiMDisc: short, linear motif discovery, correcting for
913 common evolutionary descent. *Nucleic Acids Research* **34** 3546–3554.
914 (doi:10.1093/nar/gkl486)

915 Edwards R 2019 BUSCOMP: BUSCO compilation and comparison – Assessing completeness in
916 multiple genome assemblies. *F1000Research* 8:995 (slides).
917 (doi:10.7490/f1000research.1116972.1)

918 Edwards RJ, Tuipulotu DE, Amos TG, O'Meally D, Richardson MF, Russell TL, Vallinoto M, Carneiro M,
919 Ferrand N, Wilkins MR *et al.* 2018 Draft genome assembly of the invasive cane toad, Rhinella
920 marina. *GigaScience* **7**. (doi:10.1093/gigascience/giy095)

921 Edwards RJ, Field MA, Ferguson JM, Dudchenko O, Keilwagen J, Rosen BD, Johnson GS, Rice ES,
922 Hillier LD, Hammond JM *et al.* 2021 Chromosome-length genome assembly and structural
923 variations of the primal Basenji dog (Canis lupus familiaris) genome. *BMC Genomics* **22** 188.
924 (doi:10.1186/s12864-021-07493-6)

925 Feare CJ 1985 *The Starling*. Shire.

926 Field MA, Rosen BD, Dudchenko O, Chan EKF, Minoche AE, Edwards RJ, Barton K, Lyons RJ, Tuipulotu
927 DE, Hayes VM *et al.* 2020 Canfam_GSD: De novo chromosome-length genome assembly of
928 the German Shepherd Dog (Canis lupus familiaris) using a combination of long reads, optical
929 mapping, and Hi-C. *GigaScience* **9**. (doi:10.1093/gigascience/giaa027)

930 Flynn JM, Hubley R, Goubert C, Rosen J, Clark AG, Feschotte C & Smit AF 2020 RepeatModeler2 for
931 automated genomic discovery of transposable element families. *Proceedings of the National*
932 *Academy of Sciences* **117** 9451–9457. (doi:10.1073/pnas.1921046117)

933 Griffin DK, Robertson LBW, Tempest HG & Skinner BM 2007 The evolution of the avian genome as
934 revealed by comparative molecular cytogenetics. *Cytogenetic and Genome Research* **117** 64–
935 77. (doi:10.1159/000103166)

936 Gs S & E B 2005 Automated generation of heuristics for biological sequence comparison. *BMC*
937 *Bioinformatics* **6** 31–31. (doi:10.1186/1471-2105-6-31)

938 Gu Z, Gu L, Eils R, Schlesner M & Brors B 2014 circlize Implements and enhances circular visualization
939 in R. *Bioinformatics (Oxford, England)* **30** 2811–2812. (doi:10.1093/bioinformatics/btu393)

940 Hirsch CN, Foerster JM, Johnson JM, Sekhon RS, Muttoni G, Vaillancourt B, Peñagaricano F, Lindquist
941 E, Pedraza MA, Barry K *et al.* 2014 Insights into the Maize Pan-Genome and Pan-
942 Transcriptome. *The Plant Cell* **26** 121–135. (doi:10.1105/tpc.113.119982)

943 Hofmeister NR, Werner SJ & Lovette IJ 2019 Environment but not geography explains genetic
944 variation in the invasive and largely panmictic European starling in North America. *BioRxiv*
945 643858. (doi:10.1101/643858)

946 Hofmeister NR, Stuart K, +, Rollins LA & Clayton DF 2020 Replicated invasions by starlings reveal
947 hotspots of natural selection. *Unpublished*.

948 Holt C & Yandell M 2011 MAKER2: an annotation pipeline and genome-database management tool
949 for second-generation genome projects. *BMC Bioinformatics* **12** 491. (doi:10.1186/1471-
950 2105-12-491)

951 Hunt M, Kikuchi T, Sanders M, Newbold C, Berriman M & Otto TD 2013 REAPR: a universal tool for
952 genome assembly evaluation. *Genome Biology* **14** R47. (doi:10.1186/gb-2013-14-5-r47)

953 Hyatt D, Chen G-L, LoCascio PF, Land ML, Larimer FW & Hauser LJ 2010 Prodigal: prokaryotic gene
954 recognition and translation initiation site identification. *BMC Bioinformatics* **11** 119.
955 (doi:10.1186/1471-2105-11-119)

956 Jayakumar V & Sakakibara Y 2019 Comprehensive evaluation of non-hybrid genome assembly tools
957 for third-generation PacBio long-read sequence data. *Briefings in Bioinformatics* **20** 866–876.
958 (doi:10.1093/bib/bbx147)

959 Keilwagen J, Hartung F, Paulini M, Twardziok SO & Grau J 2018 Combining RNA-seq data and
960 homology-based gene prediction for plants, animals and fungi. *BMC Bioinformatics* **19** 189.
961 (doi:10.1186/s12859-018-2203-5)

962 Koch AJ, Munks SA & Spencer C 2009 Bird use of native trees retained in young eucalypt plantations:
963 species richness and use of hollows. *Wildlife Research* **36** 581–591. (doi:10.1071/WR09037)

964 Kono N & Arakawa K 2019 Nanopore sequencing: Review of potential applications in functional
965 genomics. *Development, Growth & Differentiation* **61** 316–326.
966 (doi:https://doi.org/10.1111/dgd.12608)

967 Korf I 2004 Gene finding in novel genomes. *BMC Bioinformatics* **5** 59. (doi:10.1186/1471-2105-5-59)

968 Kuo RI, Cheng Y, Zhang R, Brown JWS, Smith J, Archibald AL & Burt DW 2020 Illuminating the dark
969 side of the human transcriptome with long read transcript sequencing. *BMC Genomics* **21**
970 751. (doi:10.1186/s12864-020-07123-7)

971 Levy Karin E, Mirdita M & Söding J 2020 MetaEuk—sensitive, high-throughput gene discovery, and
972 annotation for large-scale eukaryotic metagenomics. *Microbiome* **8** 48. (doi:10.1186/s40168-
973 020-00808-x)

974 Li H 2018 Minimap2: pairwise alignment for nucleotide sequences. *Bioinformatics (Oxford, England)*
975 **34** 3094–3100. (doi:10.1093/bioinformatics/bty191)

976 Linz GM, Homan HJ, Gaulker SM, Penry LB & Bleier WJ 2007 European starlings: A review of an
977 invasive species with far-reaching impacts. *Managing Vertebrate Invasive Species*.

978 Linz G, Johnson R & Thiele J 2017 European Starlings. In *Ecology and Management of Terrestrial*
979 *Vertebrate Invasive Species in the United States*, 1st ed, pp 311–332. Ed WC Pitt. Boca
980 Raton : Taylor & Francis, 2018. | "A CRC title, part of the Taylor & Francis imprint, a member
981 of the Taylor & Francis Group, the academic division of T&F Informa plc.": CRC Press.
982 (doi:10.1201/9781315157078-15)

983 Ma Z (Sam), Li L, Ye C, Peng M & Zhang Y-P 2019 Hybrid assembly of ultra-long Nanopore reads
984 augmented with 10x-Genomics contigs: Demonstrated with a human genome. *Genomics* **111**
985 1896–1901. (doi:10.1016/j.ygeno.2018.12.013)

986 Mapleson D, Garcia Accinelli G, Kettleborough G, Wright J & Clavijo BJ 2017 KAT: a K-mer analysis
987 toolkit to quality control NGS datasets and genome assemblies. *Bioinformatics* **33** 574–576.
988 (doi:10.1093/bioinformatics/btw663)

989 Marçais G & Kingsford C 2011 A fast, lock-free approach for efficient parallel counting of occurrences
990 of k-mers. *Bioinformatics* **27** 764–770. (doi:10.1093/bioinformatics/btr011)

991 Mirarab S, Nguyen N & Warnow T 2012 SEPP: SATé-enabled phylogenetic placement. *Pacific*
992 *Symposium on Biocomputing. Pacific Symposium on Biocomputing* 247–258.
993 (doi:10.1142/9789814366496_0024)

994 O'Connor RE, Kiazim L, Skinner B, Fonseka G, Joseph S, Jennings R, Larkin DM & Griffin DK 2019
995 Patterns of microchromosome organization remain highly conserved throughout avian
996 evolution. *Chromosoma* **128** 21–29. (doi:10.1007/s00412-018-0685-6)

997 Palacio FX, Maragliano RE & Montalti D 2016 Functional role of the invasive European Starling,
998 Sturnus vulgaris, in Argentina. *Emu* **116** 387–393. (doi:10.1071/MU16021)

999 Peona V, Weissensteiner MH & Suh A 2018 How complete are "complete" genome assemblies?—An
1000 avian perspective. *Molecular Ecology Resources* **18** 1188–1195.
1001 (doi:https://doi.org/10.1111/1755-0998.12933)

1002 Phair DJ, Roux JJL, Berthouly-Salazar C, Visser V, Vuuren BJ van, Cardilini APA & Hui C 2018 Context-
1003 dependent spatial sorting of dispersal-related traits in the invasive starlings (Sturnus
1004 vulgaris) of South Africa and Australia. *BioRxiv* 342451. (doi:10.1101/342451)

1005 Prentis PJ, Wilson JRU, Dormontt EE, Richardson DM & Lowe AJ 2008 Adaptive evolution in invasive
1006 species. *Trends in Plant Science* **13** 288–294. (doi:10.1016/j.tplants.2008.03.004)

1007 Quinlan AR & Hall IM 2010 BEDTools: a flexible suite of utilities for comparing genomic features.
1008 *Bioinformatics* **26** 841–842. (doi:10.1093/bioinformatics/btq033)

1009 Rhie A, McCarthy SA, Fedrigo O, Damas J, Formenti G, Koren S, Uliano-Silva M, Chow W,
1010 Fungtammasan A, Gedman GL *et al.* 2020 Towards complete and error-free genome
1011 assemblies of all vertebrate species. *BioRxiv* 2020.05.22.110833.
1012 (doi:10.1101/2020.05.22.110833)

1013 Rice P, Longden I & Bleasby A 2000 EMBOSS: the European Molecular Biology Open Software Suite.
1014 *Trends in Genetics: TIG* **16** 276–277. (doi:10.1016/s0168-9525(00)02024-2)

1015 Richardson MF, Sherwin WB & Rollins LA 2017 De Novo Assembly of the Liver Transcriptome of the
1016 European Starling, Sturnus vulgaris. *Journal of Genomics* **5** 54–57. (doi:10.7150/jgen.19504)

1017 Rintala J, Tiainen J & Pakkala T 2003 Population trends of the Finnish starling Sturnus vulgaris,
1018 1952—1998, as inferred from annual ringing totals. *Annales Zoologici Fennici* **40** 365–385.

1019 Robinson RA, Siriwardena GM & Crick HQP 2005 Status and population trends of Starling Sturnus
1020 vulgaris in Great Britain. *Bird Study* **52** 252–260. (doi:10.1080/00063650509461398)

1021 Rosenberg KV, Dokter AM, Blancher PJ, Sauer JR, Smith AC, Smith PA, Stanton JC, Panjabi A, Helft L,
1022 Parr M *et al.* 2019 Decline of the North American avifauna. *Science* **366** 120–124.
1023 (doi:10.1126/science.aaw1313)

1024 Sherman RM & Salzberg SL 2020 Pan-genomics in the human genome era. *Nature Reviews Genetics*
1025 **21** 243–254. (doi:10.1038/s41576-020-0210-7)

1026 Simão FA, Waterhouse RM, Ioannidis P, Kriventseva EV & Zdobnov EM 2015 BUSCO: assessing
1027 genome assembly and annotation completeness with single-copy orthologs. *Bioinformatics*
1028 *(Oxford, England)* **31** 3210–3212. (doi:10.1093/bioinformatics/btv351)

1029 Smit A, Hubley R & Green P 2013 *RepeatMasker Open-4.0*.

1030 Spooner FEB, Pearson RG & Freeman R 2018 Rapid warming is associated with population decline
1031 among terrestrial birds and mammals globally. *Global Change Biology* **24** 4521–4531.
1032 (doi:https://doi.org/10.1111/gcb.14361)

1033 Stanke M & Morgenstern B 2005 AUGUSTUS: a web server for gene prediction in eukaryotes that
1034 allows user-defined constraints. *Nucleic Acids Research* **33** W465–W467.
1035 (doi:10.1093/nar/gki458)

1036 Steinegger M & Söding J 2017 MMseqs2 enables sensitive protein sequence searching for the
1037 analysis of massive data sets. *Nature Biotechnology* **35** 1026–1028. (doi:10.1038/nbt.3988)

1038 Stuart KC, Cardilini APA, Cassey P, Richardson MF, Sherwin W, Rollins LA & Sherman CDH 2020
1039 Signatures of selection in a recent invasion reveals adaptive divergence in a highly vagile
1040 invasive species. *Molecular Ecology* **n/a**. (doi:10.1111/mec.15601)

1041 UniProt Consortium 2019 UniProt: a worldwide hub of protein knowledge. *Nucleic Acids Research* **47**
1042 D506–D515. (doi:10.1093/nar/gky1049)

1043 Vernikos G, Medini D, Riley DR & Tettelin H 2015 Ten years of pan-genome analyses. *Current Opinion*
1044 *in Microbiology* **23** 148–154. (doi:10.1016/j.mib.2014.11.016)

1045 Walker BJ, Abeel T, Shea T, Priest M, Abouelliel A, Sakthikumar S, Cuomo CA, Zeng Q, Wortman J,
1046 Young SK *et al.* 2014 Pilon: An Integrated Tool for Comprehensive Microbial Variant
1047 Detection and Genome Assembly Improvement. *PLOS ONE* **9** e112963.
1048 (doi:10.1371/journal.pone.0112963)

1049 Weisenfeld NI, Kumar V, Shah P, Church DM & Jaffe DB 2017 Direct determination of diploid genome
1050 sequences. *Genome Research* **27** 757–767. (doi:10.1101/gr.214874.116)

1051 Wheeler TJ & Eddy SR 2013 nhmmer: DNA homology search with profile HMMs. *Bioinformatics* **29**
1052 2487–2489. (doi:10.1093/bioinformatics/btt403)

1053 Whibley A, Kelley JL & Narum SR 2020 The changing face of genome assemblies: Guidance on
1054 achieving high-quality reference genomes. *Molecular Ecology Resources*. (doi:10.1111/1755-
1055 0998.13312)

1056 Workman RE, Myrka AM, Wong GW, Tseng E, Welch KC & Timp W 2018 Single-molecule, full-length
1057 transcript sequencing provides insight into the extreme metabolism of the ruby-throated
1058 hummingbird Archilochus colubris. *GigaScience* **7**. (doi:10.1093/gigascience/giy009)

1059 Wretenberg J, Lindström Å, Svensson S, Thierfelder T & Pärt T 2006 Population trends of farmland
1060 birds in Sweden and England: similar trends but different patterns of agricultural
1061 intensification. *Journal of Applied Ecology* **43** 1110–1120. (doi:10.1111/j.1365-
1062 2664.2006.01216.x)

1063 Xue W, Li J-T, Zhu Y-P, Hou G-Y, Kong X-F, Kuang Y-Y & Sun X-W 2013 L_RNA_scaffolder: scaffolding
1064 genomes with transcripts. *BMC Genomics* **14** 604. (doi:10.1186/1471-2164-14-604)

1065 Ye J, Zhang Y, Cui H, Liu J, Wu Y, Cheng Y, Xu H, Huang X, Li S, Zhou A *et al.* 2018 WEGO 2.0: a web
1066 tool for analyzing and plotting GO annotations, 2018 update. *Nucleic Acids Research* **46**
1067 W71–W75. (doi:10.1093/nar/gky400)

1068 Yin Z, Zhang F, Smith J, Kuo R & Hou Z-C 2019 Full-length transcriptome sequencing from multiple
1069 tissues of duck, Anas platyrhynchos. *Scientific Data* **6** 275. (doi:10.1038/s41597-019-0293-1)

1070 Yuan Y, Bayer PE, Scheben A, Chan C-KK & Edwards D 2017 BioNanoAnalyst: a visualisation tool to
1071 assess genome assembly quality using BioNano data. *BMC Bioinformatics* **18** 323.
1072 (doi:10.1186/s12859-017-1735-4)

1073

1074

1075